A *synthetic* ice core approach to estimate ion relocation in an ice field site experiencing periodical melt; a case study on Lomonosovfonna, Svalbard

C. P. Vega,[1] V. A. Pohjola,[1] E. Beaudon,[2, *] B. Claremar,[1] W. J. J. van Pelt,[1] R. Pettersson,[1] E. Isaksson,[3] T. Martma,[4] M. Schwikowski,[5] and C. E. Bøggild[6, §]

[1]{Department of Earth Sciences, Uppsala University, Villavägen 16, SE-752 36 Uppsala, Sweden}

[2]{Arctic Centre, University of Lapland, 96101 Rovaniemi, Finland}

[3]{Norwegian Polar Institute, Fram Centre 9296 Tromsø, Norway}

[4]{Institute of Geology, Tallinn University of Technology, 19086 Tallinn, Estonia}

[5]{Paul Scherrer Institut, 5232 Villigen PSI, Switzerland}

[6]{The University Centre in Svalbard, UNIS, Pb. 156 9171, Longyearbyen, Norway}

[*]{now at: Byrd Polar and Climate Research Center, 082A Scott Hall, 1090 Carmack Road, Columbus, OH 43210-1002, USA}

[§]{now at: Arctic Technology Centre, Technical University of Denmark, Kemitorvet, Bygning 204, 2800 Kgs. Lyngby, Denmark}

Correspondence to: C. P. Vega (carmen.vega@geo.uu.se)

Abstract

Physical and chemical properties of four different ice cores (LF-97, LF-08, LF-09 and LF-11) drilled at Lomonosovfonna, Svalbard, were compared to investigate the effects of meltwater percolation on the chemical and physical stratigraphy of these records. A *synthetic* ice core approach was employed as reference record to estimate the ionic relocation and meltwater percolation length at this site during the period 2007–2010. Using this method, a partial ion elution sequence obtained for Lomonosovfonna was $NO_3^- > SO_4^{2-}$, Mg^{2+}, Cl^-, K^+, Na^+ with nitrate being the most mobile within the snowpack. The relocation length of most of the ions was in the order of 1 m during this period. In addition, by using both a positive degree day (PDD) and a snow-energy model approaches to estimate the percentage of melt at Lomonosovfonna, we have calculated a melt percentage (MP) of the total annual

1 accumulation within the range between 48 and 70 %, for the period between 2007 and 2010
2 which is above the MP range suggested by the ion relocation evidenced in the LF-syn core
3 (i.e. MP = 30%). Using a firn-densification model to constrain the melt range, a MP of 30 %
4 was found over the same period which is consistent with the results of the synthetic ice core
5 approach, and a 45 % of melt for the last 60 years. Considering the ionic relocation lengths
6 and annual melt percentages, we estimate that the atmospheric ionic signal remains preserved
7 in recently drilled Lomonosovfonna ice cores at an annual or bi-annual resolution when
8 weather conditions were similar to those during the 2007–2010 period.

9 **Key words**: ion relocation, percolation length, melt index, ice cores.

1 Introduction

11 Pollutants produced in low- and mid-latitudes are transported to the polar regions where they
12 are included in the snow by different mechanisms, mainly wet and dry deposition,
13 accumulating in glaciers and ice caps. Major ions, such as SO_4^{2-}, NO_3^-, Na^+, and Cl^-, are
14 deposited in the snowpack and can be measured in ice cores, providing valuable information
15 about their sources, chemical transformations in the atmosphere, and transport patterns to the
16 sampling site (*Laj et al.*, 1992; *Goto-Azuma and Koerner*, 2001; *Kekonen et al.*, 2002;
17 *Hastings et al.*, 2004; *Hastings et al.*, 2009). Nitrate (NO_3^-), for example, has been used as a
18 record for past atmospheric nitrogen oxides ($NO_x = NO_2 + NO$) (*Kekonen et al.*, 2002;
19 *Röthlisberger et al.*, 2002; *Hastings et al.*, 2005; *Hastings et al.*, 2009; *Vega et al.*, 2015b).
20 However, this proxy has been difficult to develop since NO_3^- in snow has several sources and
21 experiences post-depositional processes, such as photolysis, diffusion within the ice,
22 evaporation as HNO_3, or relocation by meltwater (*Goto-Azuma et al.*, 1994; *Honrath et al.*,
23 1999; *Rempel et al.*, 2002; *Röthlisberger et al.*, 2002). The latter has been an enigma to
24 potential ice core sites since relocation and preferential elution of chemical species gives an
25 altitudinal and latitudinal threshold for potential drilling sites. To make use of environmental
26 data from outside the dry snow zones on glaciers in the polar areas, it is important to give
27 better regional coverage of the atmospheric chemistry outside the large polar ice sheets. For a
28 correct interpretation of the chemical ice core data from drilling sites where significant
29 summer melting occurs, it is necessary to estimate the post-depositional effects of meltwater
30 percolation on the chemical content of snow and ice.

31 It is known that most of the ice core drilling sites at Svalbard experience summer melting,
32 which may damp the chemical signal of ionic species, making it difficult to understand the

transfer function between ion concentrations in the atmosphere and the snow (*Goto-Azuma et al.*, 1994; *Isaksson et al.*, 2001; *Moore et al.*, 2005; *Grinsted et al.*, 2006). Ions do not move uniformly when are removed from the snowpack by meltwater. Instead, they are released following a preferential elution (*Goto-Azuma et al.*, 1994; *Eichler et al.*, 2001; *Ginot et al.*, 2010). The elution of ions is a consequence of sequential grain-scale processes during dry metamorphism (*Brimblecombe et al.*, 1985; *Schöndorf and Herrmann*, 1987; *Goto-Azuma et al.*, 1994) and also influenced by the pH of meltwater (*Goto-Azuma et al.*, 1994). *Moore and Grinsted* (2009) calculated the elution factors (*e*) of several ions present in snow and ice from an ice core drilled at Lomonosovfonna, Svalbard during 1997 (LF-97). According to their results, the most mobile species in the snow were Ca^{2+}, Mg^{2+}, SO_4^{2-} and NO_3^- with Na^+, Cl^-, NH_4^+ and K^+ being eluted later. The elution sequence changed slightly in ice, where NO_3^- is the most mobile specie and Mg^{2+} the latest ion to elute. *Moore and Grinsted* (2009), *Ginot et al.* (2010) and *Eichler et al.* (2001) results point to the ionic charge as the control factor in the elution process instead of the acidic character of the ion as reported by *Brimblecombe et al.* (1985) and *Goto-Azuma et al.* (1994).

The special characteristics of snow and firn properties on high altitude ice fields with heterogeneous stratigraphy as Lomonosovfonna are a consequence of the long winter season with air temperatures below the freezing point, enhanced snow drift by strong winds, relatively low annual snow accumulation and cold ground surfaces, punctuated by intermittent melt events. The interaction between the meltwater front formed during episodic melt events and the different stratigraphic horizons form preferential flow patterns and create a secondary stratigraphy if refreezing takes place within colder layers (*Colbeck*, 1991). The secondary stratigraphy produced by refreezing water will have a large influence in meltwater flow and discharge (*Bøggild*, 2000). During the intermittent melt periods, dislocation of water from more superficial layers percolates into the deeper stratigraphy routed as preferential meltwater flow and the formation of solute enriched ice layers during refreeze of the percolated water will affect the chemistry (i.e. ionic concentrations in this study) recorded in ice cores drilled at the high altitude ice fields of Svalbard.

One estimate to measure if snow melting and percolation have occurred in an ice core stratigraphy is to construct an ion ratio, based on the selection of a pair of ions that originate from the same source but have dissimilar elution coefficients, e.g. Na^+/Mg^{2+} and Cl^-/K^+ as reported by *Iizuka et al.* (2002) and *Grinsted et al.* (2006). Using the logarithms of the

different ionic ratios as melt indices, denoted as W_{NaMg} or W_{ClK} depending upon the pair of ions selected, a reconstruction of the melting history of a particular ice core site can be reconstructed (*Grinsted et al.*, 2006). *Pohjola et al.* (2002) found that at Lomonosovfonna, about 25 % to 55 % of the annual accumulation over the 20th century may melt and percolate into the underlying snow/firn. The most mobile ions reported by *Pohjola et al.* (2002) were NO_3^- and SO_4^{2-}, which presented ~50 % higher concentrations in ice compared with firn layers. On the other hand, NH_4^+ presented an even distribution between firn and ice. A percolation mechanism was proposed to have an important role in the redistribution of this specie in the ice crystals after deposition. *Pohjola et al.* (2002) concluded that although some ions may have had a high mobility within the upper part of the LF-97 ice core (0–36 m deep) during anomalously warm summers, the signal was still identifiable, being retained within an annual or biannual resolution.

The aim of this work is to study the temporal change of the snow/firn chemical and physical stratigraphy on the ice field Lomonosovfonna, Svalbard. In this study we will use data from shallow ice cores and snow pits repeatedly studied in 2008, 2009, 2010 and 2011 at Lomonosovfonna to investigate the temporal and vertical change in the stratigraphy and ion composition of the snow/firn column. To manage the sequential change in ion concentrations we will create a *synthetic* ice core using the top layer (~1 year accumulation) of different shallow ice cores and snowpits to have a reference record to assess the relocation of major ions by meltwater and the percolation length at the site during recent years. In addition, the melt percentage of the annual accumulation at Lomonosovfonna is obtained by using a positive degree day and a snow-energy model approach, and used together with the *synthetic* core to infer the effects of meltwater on the ionic signals present in recent ice cores drilled at Lomonosovfonna.

2   Methods

2.1   Study sites

Four ice cores (LF-97, LF-08, LF-09 and LF-11) and a 1.50 m deep snowpit (SP LF-10) were considered in this study, all retrieved at the Lomonosovfonna ice cap, which is one of the highest glaciated areas in Svalbard with an elevation of ~1250 m a.s.l. (*Isaksson et al.*, 2001; *Beaudon*, 2012; *Vega et al.*, 2015b) (Figure 1). Lomonosovfonna is located northeast of Longyearbyen, which is the largest settlement in Svalbard, and Pyramiden, a smaller settlement where coal mining activities were carried out until 1998. Two of the ice cores (LF-

1 97 and LF-08) were drilled at the highest point of the ice cap ca. 100 m apart from each other,

2 while the LF-09 and LF-11 ice cores were drilled ca. 4.5 km east-south-east from the site

3 cored in 1997 and 2008 (Figure 1, Table 1).

2.2 Sampling and analyses

5 The cutting, sampling and chemical analyses of the LF-97 and LF-08 ice cores are reported by

6 *Kekonen et al.* (2005, and references therein) and *Beaudon* (2012), respectively. The LF-09

7 and LF-11 ice core cutting and SP LF-10 sampling were done in clean conditions, wearing

8 clean overalls, face masks and powder free gloves. All materials employed to collect the

9 samples were rinsed with ultra-pure water (18 MΩ) and kept in clean plastic bags. Ions were

10 quantified using a Metrohm ProfIC 850 ion chromatographer; samples and standards were

11 melted and handled under laminar flow hood (class 100) to minimize any contamination from

12 the laboratory environment. Samples and standards were placed in the auto-sampler covered

13 with aluminium foil to avoid any dust contamination. Three sample blanks (made of ultra-

14 pure water) were analysed at the beginning and the end of every batch. Sample checks (bulk-

15 snow from Ny-Ålesund or Uppsala) were analysed every ten samples to ensure the

16 replicability of the measurements within a batch. The analytical error was below 5 % for each

17 ion. Detection limits (D.L.) for each ion were calculated as the average value of six blanks

18 plus 1.68 times the standard deviation (σ) of the six measurements (i.e.

19 $D.L. = average_{\text{blank}} + 1.68 \times \sigma_{\text{blank}}$), being below 0.3 µeq L^{-1} for all ions.

20 Water stable isotopes (δ^{18}O-H$_2$O) were analysed at the Institute of Geology at Tallinn

21 Technical University, Estonia. The measurements were done with a Picarro L2120-i water

22 isotope analyser (cavity ringdown spectroscopy technology) with a high precision vaporizer

23 A0211. All isotope measurements were calibrated in a two-point scale against the

24 international standards VSMOW (Vienna Standard Mean Ocean Water) and VSLAP (Vienna

25 *Standard* Light Antarctic Precipitation). The reproducibility of replicate analysis for δ^{18}O-

26 H$_2$O measurements was estimated to be ± 0.1 ‰.

27 The ice layer and grain size were inspected in each core section by visual examination on a

28 lighted bench located in the cold laboratory (−20 °C) at the Norwegian Polar Institute. Bulk

29 density was calculated by weighing and measuring each ice core piece of the LF-97, LF-09

30 and LF-11 cores. Density in the LF-08 core was estimated using high resolution dielectric

31 profiling (DEP) with a threshold value of 900 kg m^{-3}, i.e. values above that were set to NaNs.

1 The stratigraphic melt index was calculated as the percentage of clear ice present in the ice

2 core (considering the ice core length in m w.e. (m water equivalent)).

2.3 Synthetic ice core construction

4 In order to estimate the effects of meltwater percolation on the chemical record at

5 Lomonosovfonna, a *synthetic* ice core approach was implemented. This consists of building

6 an unperturbed ice core using only the top meter of the snowpack from different ice cores (top

7 meters of the LF-08 and LF-09 cores and the SP LF-10 snowpit), thus, constructing a snow-

8 firn record covering the previous year until the date of the sampling/drilling of the previously

9 sampled/drilled snowpit/core during the period 2007–2010 (Table 2). Consequently, summer

10 snow has been included in the synthetic core (Table 2); therefore, no error due to exclusion of

11 this layer is present in the time scale. However, the summer snow in the synthetic core has

12 most probably experienced melting at each interval, i.e. in the summer of 2009, 2008 and

13 2007, correspondently. Since each new segment of the synthetic core starts in the spring of

14 the corresponding year (Table 2), ions that could have been relocated from the summer layer

15 above are not present in the new core segment due to its different origin (Table 2).

2.4 Calculation of the meltwater

17 In order to quantify the meltwater produced at Lomonosovfonna, two independent approaches

18 were used: a simple positive degree day (PDD) model using instrumental temperature data

19 from stations near Lomonosovfonna; and a coupled snow-energy balance model (*van Pelt et*

20 *al*., 2012) that delivers snowmelt as output.

2.4.1 PDD model

22 We considered temperature instrumental data from three different sites in Svalbard:

23 Longyearbyen Airport, Sveagruva and Ny-Ålesund (data from the Norwegian Meteorological

24 Institute, http:/eklima.met.no/). To estimate the number of positive degree days (PDD) at

25 Lomonosovfonna, a lapse rate of $-0.0044\ °C\ m^{-1}$ was used (*Pohjola et al*., 2002). An annual

26 average number of 37 PDD at Lomonosovfonna was calculated when using the combined

27 temperature records of Longyearbyen Airport, Sveagruva and Ny-Ålesund (i.e. average value

28 of daily temperatures from the three stations), during the period between 1989–2010. The

29 meltwater production was calculated as described by *Pohjola et al.* (2002), using the melt

30 capacity of snow as a function of the PDD at Lomonosovfonna, considering the degree day

factor (DDF) as 3.0 mm water $°C^{-1}$ d^{-1} found at Svalbard after calibration against stake measurements (*Nuth et al.*, 2012). In a recent study by *Claremar* (2013) that employs Polar Weather Research and Forecast model (Polar WRF) (*Skamarock et al.*, 2008; *Wilson et al.*, 2011) a value for DDF of 25 mm $°C^{-1}$ d^{-1} of water was found at Lomonosovfonna. However, this DDF value has proven to be too high due to the poor modelling of the net mass balance at Lomonosovfonna when using Polar WRF temperatures and snow accumulation rates for the last decades (*Claremar*, 2013). Consequently, to calculate the meltwater we employed the DDF value proposed by Nuth et al. (2012) which is more realistic for Lomonosovfonna.

2.4.2 Coupled snow-energy balance model

The coupled model was developed to simulate the surface energy balance and subsurface conditions, in order to predict melt, refreezing and runoff at Nordenskiöldbreen, Svalbard and it is described by *van Pelt et al.* (2012) and (2014). The meltwater refreezing output of the grid point located at 1200 m a.s.l. was used in this study to account for melting at the Lomonosovfonna ice core site. At this elevation runoff does not occur; which implies that all the available water at the surface (from melt and rain) refreezes within the snow/firn pack.

3   Results and discussion

3.1   Dating of the ice cores

The LF-97 ice core has been dated by different methods (e.g. radioactive horizons, $\delta^{18}O$-H_2O cycles counting, volcanic horizons) having a time scale that covers the past 800 years (*Isaksson et al.*, 2001; *Pohjola et al.*, 2002). An updated time scale for this ice core has been recently published by *Divine et al.* (2011).

During the 2009 drilling campaign at Lomonosovfonna, two parallel ice cores were drilled: the LF-09 (36 m deep, this study) and a longer core LF-09$_{deep}$ (149.5 m deep) (*Wendl et al.*, 2015). Tritium (^3H) measurements done in the LF-09$_{deep}$ ice core estimate the 1963 ^3H horizon (*Pinglot et al.*, 1999) at 23.6 m w.e., with a resulting accumulation rate of 0.51 m y^{-1} w.e. between the ^3H radioactive horizon and the top of the ice core (*Wendl et al.*, 2015). In addition, the high resolution chemical data available for the LF-09 ice core (samples taken each 8 cm) allowed the use of a multilinear regression method (MLR) developed by *Moore et al.* (2012) to account for volcanic layers in the non-sea salt sulfate concentrations. A detailed description of the usage of the MLR method on the dating of the LF-09 ice core can be found in *Vega et al.* (2015b). In addition to the MLR method, an automated $\delta^{18}O$-H_2O

1 cycles counting routine was used in the dating. This method counted δ^{18}O-H$_2$O annual cycles

2 that had an amplitude A > 0.1 ‰ (δ^{18}O uncertainty in the SMOW scale) and a frequency in

3 the sub-annual cycle (λ_{seas}) larger than 1/3 the accumulation rate (*Pohjola et al.*, 2002). Using

4 both methods, the time scale for the LF-09 core was estimated to span between 1957–2009

5 (*Vega et al.*, 2015b).

6 The LF-08 and LF-11 ice cores were dated using the automated δ^{18}O-H$_2$O annual cycles

7 counting routine and by comparing the Cl$^-$ record with the respective LF-09 ice core profile.

8 The LF-08 core data has only been interpreted between the top and 6.4 m due to the presence

9 of an anomalous column of clear ice between 6.4 m and 10.6 m deep which is suspected to be

10 originated by a water-filled crevasse. Clear ice layers of this length have never been observed

11 in any of our ice coring efforts. The summit has a few, but deeply cutting extensional

12 crevasses not visible under the snow cover in the spring. The time scales for the cores were

13 estimated to cover the 2000–2008 and 2004–2011 periods for the LF-08 and LF-11 (*Vega et*

14 *al.*, 2015a) ice cores, respectively.

15 The time scale of the SP LF-10 snowpit was obtained by assuming a constant snow

16 accumulation rate over the depth-scale, resulting in time coverage between 2009.4–2010.4.

17 **3.2   Major ions**

18 All the ionic concentrations were binned to annual averages to obtain equally spaced time

19 series of one year resolution, which can be compared in between the different ice cores.

20 Having all the chemical species as annual averages, their concentrations (c_i) were normalized

21 to the mean value for each specie in each ice core record, during the total overlapping period

22 (1957–2009) to compare the variations of the ions in the different ice cores (Equation 1).

23
$$c_N = \frac{c_i - c_{mean}}{\sigma} , \qquad \text{Equation 1}$$

24 where c_N is the normalized concentration of a given ion, c_{mean} is the ion mean in the specific

25 ice core or strata, and σ is the standard deviation of the series.

26 When comparing the annual average concentrations between the different ice cores, some of

27 the peaks show a lag between the different records which likely is associated with the

28 uncertainty of the dating of the three different ice cores. We applied a 5-year moving average

29 smoothing to the annual chemical data (Figure 2). The dating error of the LF-08 and LF-09, in

1 respect to the LF-97 ice core, was estimated as ± 2 years. We found that similar temporal

2 variations experienced by the different ions were registered in the different Lomonosovfonna

3 ice cores during the overlapping period studied (Figure 2).

4 Table 3 shows the Pearson coefficient (R) and the Wilcoxon rank sum test between the

5 different species in the LF-97 and LF-09 ice cores, smoothed out with 5-year moving

6 averages of the annual data. The Wilcoxon rank sum test was also applied to the ion series in

7 the LF-08 and LF-09 cores to evaluate the hypothesis that ion concentrations in the different

8 LF-cores are samples from continuous distributions with equal medians. The *R*-values

9 between the LF-08 and LF-09 cores were not calculated since the overlapping period using 5-

10 year moving average was too short. The *R*-values and the results of the Wilcoxon test in

11 Table 3 suggest that the LF-97 and LF-09 cores, and the LF-08 and LF-09 cores have

12 comparable chemical records for all ions during the period 1956–1996 and 2000–2008,

13 respectively. Consequently, they can be used to interpret the main chemical and climatic

14 patters at Lomonosovfonna at this resolution.

15   **3.3   Ionic distribution in the snowpack**

16 In order to investigate to what degree ions are eluted from the snowpack when meltwater

17 percolates, we first compared the log-transformed concentrations (Log(c)) of the different

18 species measured in the LF-09 and LF-11 ice cores at different snowpack facies: i.e. snow,

19 ice, and firn. The chemical record of the LF-09 ice core was considered only during the period

20 2004–2009 when it overlaps with the LF-11 ice core.

21 Figure 3 shows that the median Log(c) of ions in the LF-09 ice core is significantly higher, at

22 a 95% confidence level, in the snow compared to ice and firn for SO_4^{2-}, Cl^-, NO_3^-, Br^-, Na^+

23 and K^+, with higher Log(c) values also for Ca^{2+} and Mg^{2+}, however, not significant.

24 Moreover, concentrations show similar medians in firn and ice. On the other hand, Figure 4

25 shows that median Log(c) in the LF-11 ice core are significantly higher in the snow compared

26 to both ice and firn only for Br^- and Mg^{2+}, with SO_4^{2-} median in snow being only significantly

27 higher than in ice. The rest of the ions present even concentrations in all the strata, with the

28 exception of NH_4^+ which shows a higher median concentration in ice compared to firn and

29 snow.

30 Previous work by *Pohjola et al.* (2002) focused on the effect of periodic melting in the

31 chemical record of an ice core drilled at Lomonosovfonna (LF-97) shows that the average

ionic concentrations of the different ionic species were higher in the ice facies than in the firn layers. We observed that this is only significant for NH_4^+ in the LF-11 ice core. Since all ions in the LF-09 and LF-11 ice cores within the period 2004–2011 (10 m deep) are mostly distributed between the snow and firn, we infer that ions in this section of the ice cores have not been heavily relocated by meltwater percolation. Since the amount of meltwater production at the summit of Lomonosovfonna is unknown for the studied years, three different approaches were used in order to estimate and relate it to ionic snowpack redistribution (see section 3.5.).

In order to elucidate the evolution of meltwater production over time, the chemical melt index (W_{NaMg}), defined as $Log(Na^+)/(Mg^{2+})$ (using ionic concentrations in $\mu eq\ L^{-1}$) (*Iizuka et al.*, 2002; *Grinsted et al.*, 2006) was calculated in the different Lomonosovfonna ice cores (Figure 5). This chemical approach is based on the selection of a pair of ions that have the same source but dissimilar elution coefficients within the snowpack, e.g. Na^+/Mg^{2+} and Cl^-/K^+ (*Grinsted et al.*, 2006). Positive W_{NaMg} values indicate that melting has most probably occurred. This is the case of the four Lomonosovfonna ice cores (Figure 5) which show positive melt indices during the last 60 years. As observed in Figure 5, melting at the drilling site is far from being constant; a period of particular high melt is evident during mid-1980s to mid-1990s which is concomitant with a period of relatively high number of PDDs at Lomonosovfonna. Although the above mentioned method is useful to infer melting regimes at Lomonosovfonna at large time scales (i.e. decadal to centennial), it is not suitable to infer melting at sub-, and multi-annual resolutions; therefore, the *synthetic* ice core approach described in this study presents a suitable option.

3.4 Synthetic ice core

Assuming that snowmelt does not occur during winter, and considering that precipitation records of different Svalbard sites show that most of the precipitation is registered during the winter and autumn seasons (Førland et al., 2011), it is expected that the synthetic ice core (LF-syn) captures the unperturbed chemistry of the winter, autumn, summer and early spring seasons between spring 2007–2010. Figure 6 shows the annual precipitation cycle at Longyearbyen airport and Ny-Ålesund stations and the precipitation amount and snow accumulation from the two stations and the LF-syn core during the period 2007–2011. The snow accumulation in the LF-syn core was calculated as the length (in m w.e.) between two

LF-syn core samples which in average represent 1.2 months of accumulation. Both, the meteorological and the ice core records are coherent with each other, depicting higher accumulation rates during the autumn/winter period than spring/summer. Consequently, it is expected that the LF-syn ice core is representative of the snow accumulation regime at Lomonosovfonna during 2007–2010. The flat accumulation observable during the winter 2010 is due to the assumption of a linear time scale when dating each snow layer of the snowpit dug out in 2010 (SP LF-10). In addition, the average annual mass loading of each ion was calculated for the period 1980–2009 by averaging the annual ion loads calculated in the LF-97 and LF-09 cores. This procedure averaged out the possible effects of percolation and relocation of ions between the strata corresponding to different years. This estimate was then compared with the mass loading of the different ions corresponding to individual years in the LF-syn core (i.e. 2007–2010) which are assumed to represent cumulative autumn-winter-early spring snow accumulation unaltered by meltwater percolation or ion relocation. It was found that the 5-year LF-syn record represents between 70–200 % of the 30-year average ion mass loading with NH_4^+ and Mg^{2+} located at the bottom and top percentage boundaries, respectively, and NO_3^- and SO_4^{2-} representing 94 % and 111 % of the average, respectively. Keeping in mind that the mass loading for most of the ions show increasing values since 2005 (not shown), thus, influencing the percentage of average mass loading in the LF-syn core, we consider that this synthetic core is adequate to investigate ion relocation during the period 2007–2011. The LF-syn core was then compared with the LF-11 core to evaluate the effects of ion elution/deposition between 2007–2010 (recorded in the LF-11 ice core) compared to the unperturbed LF-syn ice core (Figure 7). Since the top part of the LF-11 core (0– 0.6 m w.e.) was not used to construct the LF-syn core (Table 2) and to avoid any bias caused for the snow accumulated after the spring 2010 and 2011, this period was not considered in the normalization of the LF-11 ionic concentrations. Figure 7 shows that the LF-11 record has noticeable large c_N peaks, e.g. around summer 2009, that can be associated with the increase in ionic concentrations by the relocation of ions by the refreezing of percolation water. Figure 8 shows the differences between c_N in both ice cores (LF-11 − LF-syn) calculated after interpolating the records at 0.01-year time steps to homogenize the data. A lowpass filter (half-year moving average) was used to filter out high frequency processes superimposed to the percolation and relocation effect (Figure 8); consequently, a cutting threshold of half a year was assumed for the relocation of ions. Using the filtered time series shown in Figure 8, we considered a relocation period when the differences in c_N are positive. Positive differences

1 indicate higher ionic concentrations in the LF-11 ice core with respect to the LF-syn ice core,

2 therefore, ice-firn layers enhanced in ions due to relocation by percolation water. Negative

3 differences indicate ionic elution happening at that layer. Consequently, the study period was

4 divided in four sub-periods denoted with roman numbers (Figure 8). It is worth saying, that

5 even though the LF-11 core was used for comparison with the LF-syn core only between

6 2007.4–2010.4, the effects of melt water produced and percolated during the summer of 2010

7 are recorded in the LF-11 core. Consequently, Period I encompasses the melting season of the

8 summer-spring months of 2010 (elution period). Period II reflects the deposition period after

9 the spring-summer of 2010. Period III represents elution occurred between summer of 2009

10 and summer of 2008; and Period IV encompasses a deposition period from spring of 2008 to

11 spring of 2007. From Figure 8 it can be observed that most of ions (with the exception of

12 NH_4^+ and Ca^{2+}) share similar elution/deposition features in Periods I–IV. We estimate a

13 *minimum* ionic relocation length as the difference in depth between the minimum/maximum

14 (elution/deposition) c_N peaks observed in Periods I–II (Figure 8, Table 4). The difference was

15 not calculated in Periods III–IV since the time series are truncated before reaching a

16 maximum value, however the elution minima are noted in Table 4. The relocation length was

17 calculated for all ions, with the exception of NH_4^+ and Ca^2.

18 Considering the elution/deposition c_N peaks estimated above, a partial ionic elution scheme at

19 Lomonosovfonna for the period 2007–2010 can be inferred, resulting in NO_3^- being the most

20 mobile ion. This partial elution scheme agrees with previous studies done at Lomonosovfonna

21 (*Moore and Grinsted*, 2009) which found that NO_3^- was highly mobile. The partial elution

22 sequence and ion relocation lengths shown in Table 4, suggest that the ions are relocated by

23 meltwater at short lengths, probably trapped in thin and medium-thick ice layers present

24 within the ice column observable in the LF-97, LF-09 and LF-11 cores (Figure 9), or in

25 refrozen water that soaks the firn column filling the pore space. Nevertheless, the results

26 shown in Figure 8 and Table 4 are not absolute for the full length of the Lomonosovfonna

27 core but rather the case for years with apparently moderate melting (e.g. MP<50%). In years

28 were summers are warmer and/or longer, ions may percolate further down in the snowpack

29 and get trapped in medium-thick to thick ice layers which start to form at about 3–10 m deep

30 in the ice column as observable in the LF-97 and LF-09 cores (Figure 9).

31 The *synthetic core* idea was also tested in Greenland snowpit data of the Core Atmospheric

32 Measurements at Summit, Greenland Environmental Observatory project available at the

33 ACADIS   Gateway   data   repository

We selected two snowpits from Summit: one sampled on July 1st 2012 and the other one sampled in July 27th 2012 (after the melt event of July 12th 2012). We used the density profile and the chemistry record to find an appropriate and realistic match between the ion series. The comparison of the density profiles is shown in Figure 10. The depth scale of the snowpit sampled in July 27th was adjusted to find a reasonable match with the density profile of the snowpit samples in July 1st. It was necessary to shift the depth profile by 3 cm which is realistic for the interval of 1 month between the sampling and the amount of water that could have melted in mid-July at the site. According to Nghiem et al. (2012), the melt event reported at Greenland on July 12th created a 2 cm ice crust at the surface of the snowpack at Summit, which is evidenced in the density profile in Figure 10 (dashed line). Therefore, there is no evidence of intense melt at this site that could have generated melt water that percolated further down the snowpack. Therefore, we applied our method by comparing the snowpit sampled in late July with the snowpit sampled in July 1st. Following exactly the same methodology applied to Lomonosovfonna (with the exception of using the depth scale instead of the time scale), the ion normalized concentrations in the snowpits were calculated and shown in Figure 11. The ionic record is spiky, as expected for any record of this kind, especially if no melting and percolation occurs. We proceeded then to calculate the difference between the snowpit sampled in July 27th (analogous to the LF-11 core) and the snowpit sampled in July 1st (analogous to the LF-syn unperturbed core). We also filtered out high frequency variations using a lowpass filter (half-year moving average), as we did with the Lomonosovfonna data. The results are shown in Figure 12. As it can be observed in Figure 12, the filtered series do not deviate from the mean value of the concentrations, therefore, no percolation can be inferred from them, as it can be expected to be the case for Summit during the period selected. We therefore consider that our method is applicable in Svalbard cores since it does not show false positives for the Greenland snowpits.

In order to estimate how the ionic relocation length during 2007–2010 is connected to meltwater percolation length and snowpack melting, we have estimated the melt percentage at Lomonosovfonna using two different methods, as shown in the following section.

3.5 Meltwater production at Lomonosovfonna

The produced meltwater obtained by using the PDD and snow-energy model approaches are shown in Figure 13 for the period 1979–2012 (calculated using PDD and instrumental

1   temperatures), and 1989–2010 (using the snow-energy model). The production of meltwater

2   at the summit of Lomonosovfonna has increased at a rate of +0.0011 m y^{-1} w.e toward the last

3   decades (corresponding to the linear trend of meltwater production calculated with the PDD

4   and instrumental temperatures approach, Figure 13). The average melting between 1989–2010

5   was calculated as 0.17 m w.e. when using the PDD and instrumental temperature approach.

6   When considering the period between 2007–2010 (Figure 14), the melting shows alternating

7   warm and cold years (2007/2009, and 2008/2010, respectively), with meltwater average

8   values of 0.19 m w.e. and 0.27 m w.e. when using the instrumental temperatures, and the

9   coupled snow-energy model, respectively. Alternatively, meltwater production was also

10 calculated by using modelled temperatures obtained with the Polar WRF model at the summit

11 of Lomonosovfonna and a DDF of 3.0 mm water °C d^{-1}. An average meltwater production of

12 0.07 m w.e. and 0.05 m w.e. were obtained for the periods 1989–2010 and 2007–2010,

13 respectively when using the Polar WRF modelled temperatures. The meltwater production

14 obtained by the Polar WRF approach gives values that are significantly lower than the

15 meltwater obtained by using both the PDD and snow-energy model approaches which is a

16 consequence of the less number of PDDs per year estimated at the summit of

17 Lomonosovfonna when using the Polar WRF model (i.e. 18 PDDs per year between 1989–

18 2010) explained by the fact that the Polar WRF model produces lower surface temperatures

19 compared to the lapse-rate based temperatures at this site. Therefore, the meltwater calculated

20 by using Polar WRF modelled temperatures were not considered in this study.

21 In order to estimate the impact of melting on the snowpack ionic content at the summit of

22 Lomonosovfonna, the percentages of the annual snow accumulation that melts (Table 5) were

23 calculated using the results in Figure 13 and Figure 14 and the annual accumulation rate

24 between 2007–2010 at Lomonosovfonna obtained from the LF-09 and LF-11 cores. The melt

25 percentage (MP) obtained by using the instrumental temperatures (48% for the period 2007–

26 2010) was in the order of previously reported values of 47 % of melt during the warmest

27 years and 28 % during the coldest, during the period 1976–1995 (*Pohjola et al.,* 2002). The

28 relatively high MP values obtained in this study for the period 2007–2010 can be explained

29 by the increase in temperatures at the site with a consequent steady increase of the number of

30 PDD at the summit of Lomonosovfonna at a rate of 0.4 d y^{-1} for the period 1979–2012 in

31 which instrumental temperatures exist in all the three stations used, Sveagruva, Ny-Ålesund

32 and Longyearbyen airport; the MPs calculated using the PDD approach over the period 1979–

33 2010 show a steady increase of 1 % y^{-1} in line with the trend in decreasing the annual snow

14

1 accumulation in −0.01 m y^{-1} w.e. during the same period (accumulation data from the LF-09

2 ice core).

3 However, the calculated MPs using the PDD approach and the snow-energy do not agree with

4 the results obtained by the synthetic core approach which suggest that melting during the

5 2007–2010 period has not been high (i.e < 50 %) which is also supported by the stratigraphy

6 observed in the LF-09 and LF-11 cores (Figure 9Figure 9).

7 Due to the dissimilar results of MP obtained using the PDD and snow-energy model

8 approaches (Table 5), we compared the density profiles of the shallow ice cores used in this

9 study (LF-08, LF-09 and LF-11) with the total layer density values obtained using a simple

10 firn-densification model (*Reeh et al.*, 2005). The ice core density profiles were binned in

11 annual averages in order to be comparable with the output of the firn-densification model. As

12 described by *Reeh et al.* (2005), the model requires both annual average temperatures and

13 snow accumulation at the study site as input, which were set as −18.3 °C and 0.39 m w.e.,

14 according to instrumental temperatures from Sveagruva, Svalbard Airport and Ny-Ålesund

15 (the lapse rate employed to calculate the temperatures at the Lomonosovfonna summit was

16 −0.0044 °C m^{-1}), and average accumulation rates obtained from the LF-09 and LF-11 ice

17 cores, respectively, for the period between 2007–2010. The firn-densification model also

18 requires the surface snow density, which was set as 350 kg m^{-3}, and a defined spatial

19 resolution, set as 0.5 m. The firn-densification model considers the percentage of melting as

20 one of the input variables, showing output density values versus depth. Output densities of

21 900 kg m^{-3} are expected when the percentage of melt reaches 100 %. Four different melt

22 scenarios where considered: MP equal to a) 20 %, b) 30 %, c) 45 %, and d) 70 %. The results

23 of the comparison between the real ice core density profiles and the output of the firn-

24 densification model are shown in Figure 15.

25 According to Figure 15, the firn-densification model shows better agreement with the

26 measured density profiles in the top 10 m when the MP was set between 20 % and 30 %. This

27 agrees with the physical melt index of the LF-09 ice core (22 %), calculated as the percentage

28 of clear ice present in the ice core (considering the ice core length in m w.e.). However, the

29 agreement between the firn-densification model and the density profiles is poor for depths

30 deeper than 10 m (Figure 15 a–b) considering this range or MP. Figure 15 c–d, show the

31 comparison between the firn-densification model and the density profiles using a MP of 45 %

32 and 70 %. The agreement between the model and the measurements is better through the

1 whole depth profile when setting the MP to 45 % (Figure 15 c). This agrees with the physical

2 melt index of the LF-97 ice core (50 %), calculated between 1957 and 1997, however, it is not

3 consistent with the physical melt index of the LF-09 ice core (25 %), calculated for the same

4 period.

5 Considering the results shown in Table 5 and the firn-densification model output shown in

6 Figure 15 a–d, it is plausible to think that the MP at Lomonosovfonna is not straight forward

7 to estimate either using a simple PDD or the snow-energy model approach. Moreover, the use

8 of Polar WRF temperatures at Lomonosovfonna as input to obtain the MP at the site is ruled

9 out since it predicts MP values considerably lower than the values suggested by the density

10 profiles both measured and modelled (i.e. an average MP of 12 % for the period 2007–2010

11 when Polar WRF modelled temperatures and a DDF of 3.0 mm water $°C\ d^{-1}$ are used to

12 calculate the meltwater production). It also needs to be considered that the firn-densification

13 model assumes a constant melt index during the ice core time span. Therefore, the firn-

14 densification model does not include the variability in meltwater production at

15 Lomonosovfonna through time which is key to the understanding of ion relocation within the

16 snowpack at long time scales; however, the MP estimated here are suitable to understand the

17 ionic relocation and water percolation during the period 2007–2010.

18 Figure 16 shows a comparison between the LF-11 and the LF-syn ice core depth–time scale.

19 It is clear from Figure 16 that the depth differences between the ice cores (black and grey

20 lines) can be related to a partial melting of the snowpack and refreezing of the meltwater

21 taking place between the 2007–2011 period, as evidenced by the ionic relocation. An estimate

22 of the decrease in depth of the LF-syn ice core by the effects of snowpack melting considering

23 a MP = 20, 30, 48 and 70 % during 2007–2010 as suggested by the firn-densification model,

24 MPs obtained using the PDD approach (using instrumental temperatures) and the snow-

25 energy model is shown in Figure 16. It can be observed that a MP = 20–30 % results in a LF-

26 syn ice core depth-time scale highly similar to the depth-time scale of the LF-11 ice core

27 during the 2007–2010 period, confirming that the MP during that period is coherent with the

28 results of the firn-densification model but not with the PDD results shown in Table 5. This

29 relatively low MP reinforces the hypothesis that during this period, ion relocation took place

30 at shallow depths (0.5–2 m) and that the meltwater percolation depth was most probably in

31 the same order, with refreezing of meltwater within the snowpack pore space or by forming

32 thin ice layers (0.03–0.15 m) (Figure 9).

4 Conclusions

By comparing different ice cores from Lomonosovfonna and using a *synthetic* ice core approach, we have been able to estimate the elution signal and relocation length of different ions measured at the study site, in order to assess the transfer function between the atmospheric ionic concentrations and the concentration in snow and ice.

Our results show good agreement between the ionic records of three different ice cores drilled during different years, using normalized concentrations and five year moving averages. Therefore, we reiterate that the different ice core records from Lomonosovfonna all share the same climatic and chemical features, despite the fact that cores have been retrieved in different years, were sampled at different resolutions, and were analysed at different laboratories. Our conclusion is that summer melting does not degrade the climatic signals.

By using the *synthetic* ice core approach, we could estimate a partial elution sequence for the summit of Lomonosovfonna, as $NO_3^- > SO_4^{2-}$, Mg^{2+}, Cl^-, K^+, Na^+, which agrees with previous reports. This elution sequence points towards the acidic ions as being the most mobile within the Lomonosovfonna snowpack. Considering the differences between the LF-11 and the LF-syn ice cores, we conclude that the relocation length of most the ions during the 2009–2010 period is in the order of 1 m, therefore, the ions are eluted and re-deposited within the annual snow layer, considering present average accumulation rate at Lomonosovfonna (i.e. < 1 m of snow per year). Consequently, using 5-year moving averages of the ionic data allows having comparable records when different ice cores are used

By using the PDD and the snow-energy model approaches to estimate the percentage of melt (MP) at Lomonosovfonna, we have estimated average annual MP in the range of 48% to 70% for the period between 2007–2010, in contrast to the lesser melting suggested by the LF-syn core for the same period. In order to constrain the MP, we have compared different density profiles obtained at the Lomonosovfonna drilling sites with a simple firn-densification model, obtaining a most probable average annual MP of 30 % for the 2007–2010 period which is consistent with the results of the synthetic ice core approach, and 45 % of melt for the last 60 years. The lower melting percentages inferred for the 2007–2010 period compared with the whole period covered by the LF.-09 core are most probably a result of a combination of relatively high snow accumulation rates and reduced PDD during the 2007–2010 period despite of the warmer conditions registered during the last decades.

Considering our findings, we conclude that despite of the warmer conditions and higher number of PDD registered at Lomonosovfonna during the last decades, the ionic signal affected by melting is retained within the same year of deposition for all major ions.

Acknowledgements

References

ACADIS, Advanced Cooperative Arctic Data and Information Service. https://nsidc.org/acadis. (last visit 2016-04-09).

Beaudon, E. 2012. Glaciochemical evidence of spatial and temporal environmental variability across Svalbard. Arctic Centre Reports 58. Lapland University Press: Rovaniemi. ISBN 978-952-484-562-5. ISSN 1235-0583.

Brimblecombe, P., Tranter, M., Abrahams, P. W., Blackwood, I., Davies, T. D., and Vincent, C. E. 1985. Relocation and preferential elution of acidic solute through the snowpack of a small, remote, high-altitude Scottish catchment. Ann. Glaciol., 7, 141–147.

Bøggild, C. E. 2000. Preferential flow and melt water retention in cold snow packs in West-Greenland. Nordic Hydrology, 31(4/5), 287–300.

Claremar, B. 2013. Relation between meso-scale climate and glacier/snow mass balance on Svalbard, Dept. Earth Sciences, Uppsala University, SVALI Technical report. http://ncoe-svali.org/xpdf/svali_report_d2-3-11_fin.pdf.

Claremar, B., Obleitner, F., Reijmer, C., Pohjola, V., Waxegård, A. et al. (2012). Applying a Mesoscale Atmospheric Model to Svalbard Glaciers. Adv. Meteorol. 321649.

Colbeck, S. C. 1991. The layered character of snow covers. Rev. Geophys., 29 (1), 81–96.

Dee, D. P., Uppala, S. M., Simmons, A. J., Berrisford, P., Poli, P., et al. (2011). The ERA-Interim reanalysis: configuration and performance of the data assimilation system. Q.J.R. Meteorol. Soc., 137: 553–597. doi:10.1002/qj.828.

Divine, D., Isaksson, E., Martma, T., Meijer, H. A. J., Moore, J., Pohjola, V., van de Wal, R. S.W., and Godtliebsen, F. 2011. Thousand years of winter surface air temperature variations in Svalbard and northern Norway reconstructed from ice-core data. Polar Res., 30, 7379, doi:10.3402/polar.v30i0.7379.

Eichler, A., Schwikowski, M., and Gäggeler, H. W. 2001. Meltwater-induced relocation of chemical species in alpine firn. Tellus, 53B, 192–203.

Førland, E. J., Benestad, R., Hanssen-Bauer, I., Haugen, J. E., and Skaugen, T. E. (2011), Temperature and precipitation development at Svalbard 1900–2100. Adv. Meteorol., 893790, doi:10.1155/2011/893790.

Ginot, P., Schotterer, U., Stichler, W., Godoi, M. A., Francou, B., and Schwikowski, M. 2010. Influence of the Tungurahue eruption on the ice core records of Chimborazo, Ecuador. The Cryosphere, 4, 561–568, doi:10.5194/tc-4-561-2010.

Goto-Azuma, K., Koerner, R. M. 2001. Ice core studies of anthropogenic sulfate and nitrate trends in the Arctic. J. Geophys. Res., 106(D5), 4959–4969.

Goto-Azuma, K., Nakawo, M., Jiankang, H., Watanabe, O., Azuma, N. 1994. Melt-induced relocation of ions in glaciers and in a seosanal snowpack. Snow and Ice covers: Interactions with the Atmosphere and Ecosystems (Proceedings of Yokohama Symposia J2, July 1993), IAHS Publ. no. 223, 287–297.

Grinsted, A., Moore, J., Pohjola, V., Martma, T., and Isaksson, E. 2006. Svalbard summer melting, continentality, and sea ice extent from the Lomonosovfonna ice core. J. Geophys. Res., 111(D07110), doi: 10.1029/2005JD006494.

Hastings, M. G., Jarvis, J. C., Steig, E. J. 2009. Anthropogenic impacts on nitrogen isotopes of ice-core nitrate. Science, 324, 1288.

Hastings, M. G., Sigman, D. M., Steig, E. J. 2005. Glacial/interglacial changes in the isotopes of nitrate from the Greenland Ice Sheet Project 2 (GISP2) ice core. Glob. Biochem. Cycles, 19, GB4024.

Hastings, M. G., Steig, E. J., Sigman, D. M. 2004. Seasonal variations in N and O isotopes of nitrate in snow at Summit, Greenland: Implications for the study of nitrate in snow and ice cores. J. Geophys. Res., 109 (D20306), doi: 10.1029/2004JD004991.

Honrath, R. E., Peterson, M. C., Guo, S., Dibb, J. E., Shepson, P. B., and Campbell, B. 1999. Evidence of NOx production within or upon Ice particles in the Greenland snowpack. Geophys. Res. Lett., 26, 695–698.

Iizuka, Y., Igarashi, M., Kamiyama, K., Motoyama, H., Watanabe, O. 2002. Ratios of Mg^{+2}/Na^+ in snowpack and ice core at Austfonna ice cap, Svalbard, as an indicator of seasonal melting. J. Glaciol., 48(162), 452–460.

Isaksson, E., Pohjola, V., Jauhiainen, T., Moore, J., Pinglot, J. F., Vaikmäe, R., van de Wal, R. S. W., Hagen, J. O., Ivask, J., Karlöf, L., Martma, T., Meijer, H. A. J., Mulvaney, R., Thomassen, M., van den Broeke, M. 2001. A new ice-core record from Lomonosovfonna,

Svalbard: viewing the 1920–97 data in relation to present climate and environmental conditions. J. Glaciol., 47(157), 335–345.

Kekonen, T., Moore, J. C., Mulvaney, R., Isaksson, E., Pohjola, V., Van De Wal, R. S. W. 2002. A 800 year record of nitrate from the Lomonosovfonna ice core, Svalbard. Ann. Glaciol., 35, 261–265.

Kekonen, T., Moore, J., Perämäki, P., Mulvaney, R., Isaksson, E., Pohjola, V., and van de Wal, R. S. W. 2005. The 800 year long ion record from the Lomonosovfonna (Svalbard) ice core. J. Geophys. Res., 110, D07304, doi: 10.1029/2004JD005223.

Laj, P., Palais, J.M., Sigurdsson, H. 1992. Changing sources of impurities to the Greenland Ice-sheet over the last 250 years. Atmos. Environ. 26, 2627–2640.

Moore, J. C., Beaudon, E., Kang, S., Divine, D., Isaksson, E., Pohjola, V. A., and van de Wal, R. S. W. 2012. Statistical extraction of volcanic sulphate from nonpolar ice cores. J. Geophys. Res., 117, D03306; DOI 10.1029/2011JD016592.

Moore, J. C., and A. Grinsted. 2009. Ion fractionation and percolation in ice cores with seasonal melting, Physics of Ice Core Records II, Supplement Issue of Low Temperature Science, 68.

Moore, J. C., Grinsted, A., Kekonen, T., and Pohjola, V. 2005. Separation of melting and environmental signals in an ice core with seasonal melt. Geophys. Res. Lett., 32, L10501, doi: 10.1029/2005GL023039.

Morrison, H., J. A. Curry, and Khvorostyanov, V. I. 2005, A new double-moment microphysics parameterization for application in cloud and climate models. Part I: Description. J. Atm. Sci., vol. 62, no. 6, 1665–1677.

Nakanishi, M. and Niino H. 2006. An Improved Mellor–Yamada Level-3 Model: Its Numerical Stability and Application to a Regional Prediction of Advection Fog, Boundary-Layer Meteorol.,vol. 119, no. 2, 397–407.

Nghiem, S. V., Hall, D. K., Mote, T. L., Tedesco, M., Albert, M. R., Keegan, K., Shuman, C. A., DiGirolamo, N. E., and Neumann, G. 2012, The extreme melt across the Greenland ice sheet in 2012. Geophysical Research Letters, 39, L20502, doi: 10.1029/2012GL053611.

Norwegian Meteorological Institute http:/eklima.met.no/. Last visited: 2015-07-31.

Nuth, C., Vikhamar, Schuler, T. V., Kohler, J., Altena, B., and Hagen, J. O. 2012. Estimating the long-term claving flux of Kronebreen, Svalbard, from geodetic elevation changes and mass-balance modelling, J. Glaciol., 58(207), 119–133.

Pinglot, J. F., Pourchet, M., Lefauconnier, B., Hagen, J. O., Isaksson, E., Vaikmäe, R., and Kamiyama, K. 1999. Accumulation in Svalbard glaciers deduced from ice cores with nuclear tests and Chernobyl reference layers. Polar Res., 18(2), 315–321.

Pohjola, V. A., Moore, J. C., Isaksson, E., Jauhiainen, T., van de Wal, R. S. W., Martma, T., Meijer, H. A. J., and Vaikmäe, R. 2002. Effect of periodic melting on geochemical and isotopic signals in an ice core from Lomonosovfonna, Svalbard. J. Geophys. Res., 107(D4), 4036, 10.1029/2000JD000149.

Reeh, N., Fisher, D. A., Koerner, R. M., aand Clausen, H. B. 2005. An empirical firn-densification model comprising ice lenses. Ann. Glaciol., 42, 101–106.

Rempel, A. W., Wettlaufer, J. S., Waddington, E. D. 2002. Anomalous diffusion of multiple impurity species: Predicted implications for the ice core climate records. J. Geophys. Res., 107(B12), doi:10.1029/2002JB001857.

Röthlisberger, R., Hutterli, M. A., Wolff, E. W., Mulvaney, R., Fischer, H., Bigler, M., Goto-Azuma, K., Hansson, M., Ruth, U., Siggaard, M-L., Steffensen, J. P. 2002. Nitrate in Greenland and Antarctic Ice cores: a detailed description of post-depositional processes. Ann. Glaciol., 35, 209–216.

Schöndorf, T., and Herrmann, R. 1987. Transport and chemodynamics of organic micropollutants and ions during snowmelt. Nordic Hydrology, 18, 259–278.

Skamarock, W. C., Klemp, J. B., Dudhia, J., Gill, D. O., Barker, D. M., Duda, M. G., Huang, X.-Y., Wang, W., and Powers, J. G. 2008. A description of the advanced research WRF version 3. NCAR/TN-475+STR, NCAR Technical Notes, Mesoscale and Microscale Meteorology Division, National Center for Atmospheric Research, Boulder, Colorado, USA.

Van Pelt, W. J. J., J. Oerlemans, C. H. Reijmer, V. A. Pohjola, R. Pettersson, and J. H. Van Angelen. 2012. Simulating melt, runoff and refreezing on Nordenskiöldbreen, Svalbard, using a coupled snow and energy balance model. The Cryosphere, 6, 641–659, doi: 10.5194/tc-6-641-2012.

1   Van Pelt, W. J. J., Pettersson, R., Pohjola, V. A., Marchenko, S., Claremar, B., and

2   Oerlemans, J. 2014. Inverse estimation of snow accumulation along a radar transect on

3   Nordenskiöldbreen, Svalbard, J. Geophys. Res. Earth Surf., 119, 816–835,

4   doi:10.1002/2013JF003040.

5   Vega, C. P., Björkman, M. P., Pohjola, V. A., Isaksson, E., Pettersson, R., Martma, T., Marca,

6   A. D, Kaiser, J. 2015a. Nitrate stable isotopes and major ions in snow and ice samples from

7   four Svalbard sites. Polar Res., 34, 23246, http://dx.doi.org/10.3402/polar.v34.23246.

8   Vega, C. P., Pohjola, V. A., Samyn, D., Pettersson, R., Isaksson, E., Björkman, M. P.,

9   Martma, T., Marca, A. D, Kaiser, J. 2015b. First Ice Core Records of Nitrate Stable Isotopes

10 from Lomonosovfonna, Svalbard. J. Geophys. Res. Atmos., 120, doi:10.1002/2013JD020930.

11 Wendl, I. A., Eichler, A., Isaksson, E., Martma, T., and Schwikowski, M. 2015. 800 year ice-

12 core record of nitrogen deposition in Svalbard linked to ocean productivity and biogenic

13 emissions. Atmos. Chem. Phys., 15, 7287–7300, doi:10.5194/acp-15-7287-2015.

14 Wilson, A. B., D. H. Bromwich, K. M. Hines. 2011. Evaluation of Polar WRF forecasts on

15 the Arctic System Reanalysis domain: Surface and upper air analysis. J. Geophys. Res., 116,

16 D11112, doi: 10.1029/2010JD015013.

17

1 **Tables**

2 Table 1 Drilling site and ice core description for the three different cores used in this study.

Ice core	Drilling date	Location	Elevation (m a.s.l.)	Length (m)	Reference
LF-97	May 1997	78° 51' N 17° 25' E	1250	121.6	Isaksson et al. (2001)
LF-08	Mar. 2008	78° 51' N 17° 24' E	1250	10.6	Beaudon (2012)
LF-09	Mar. 2009	78° 49' N 17° 25' E	1200	36.0	Vega et al. (2015b)
SP LF-10	Mar. 2010	78° 49' N 17° 25' E	1200	1.5	This work
LF-11	Apr. 2011	78° 49' N 17° 25' E	1200	7.6	Vega et al. (2015a)

3

1 Table 2 *Synthetic* ice core construction using the different Lomonosovfonna shallow cores

2 (LF-08 and LF-09) and SP LF-10 snowpit. *The top meter of the LF-11 was not used to

3 construct the *synthetic* ice core but it is shown here as reference to account for the final depth

4 of the *synthetic* core.

Ice core	Depth interval (m w.e.)	Time interval (year)
LF-11*	0.0–0.6	2011.4–2010.4
SP LF-10	0.6–1.4	2010.4–2009.3
LF-09	1.4–1.8	2009.3–2008.3
LF-08	1.8–2.3	2008.3–2007.4

1   Table 3 Top table: Pearson coefficients (R) and Wilcoxon rank sum test results (p-values), at a
2   95 % confidence interval, between the different ions measured in the LF-97 and LF-09 ice
3   cores (normalized concentrations and smoothed out as 5-year running averages). The
4   overlapping period is 1957–1996 (top table). p-values of the Pearson correlation have been
5   corrected for the reduced degrees of freedom introduced by the 5-year smoothing. Significant
6   values (correlation, $p < 0.05$; Wilcoxon rank sum test $p > 0.05$) are shown in italics. Bottom
7   Table: Wilcoxon rank sum test at a 95 % confidence interval between the different ions
8   measured in the LF-08 and LF-09 ice cores (normalized concentrations and smoothed out as
9   5-year running averages). The overlapping period is 2000–2008. N represents the sample size.

LF-97 and LF-09 ice cores								
Ion	Cl^-	NO_3^-	SO_4^{2-}	Na^+	NH_4^+	K^+	Ca^{2+}	Mg^{2+}
R (N=36	*0.46*	*0.64*	*0.56*	*0.49*	*0.77*	*0.66*	0.36	*0.72*
Wilcoxon rank sum test (p-value, N=36)	*0.32*	*0.13*	*0.35*	*0.16*	*0.15*	*0.61*	*1.00*	*0.34*
LF-08 and LF-09 ice cores								
Wilcoxon rank sum test (p-value) (N=5)	*0.84*	*0.10*	*0.22*	*0.55*	0.02	*0.69*	*1.00*	*0.10*

10

1   Table 4 Minimum relocation length estimated for each ion measured in the LF-11 ice core.

Ion	SO_4^{2-}	Mg^{2+}	Cl^-	K^+	Na^+	NO_3^-
Periods I–II: Relocation length (m)	1	1	1	1	1	1.2
Deposition maximum (year)	2009.76	2009.76	2009.76	2009.76	2009.76	2009.61
Periods III-IV Elution minimum (year)	2008.18	2008.66	2008.76	2008.76	2008.76	2008.18

2

1 Table 5 Percentages of melted annual snow accumulation (MP) calculated with the PDD

2 approach (*Pohjola et al*., 2002; *Nuth et al*., 2012) using instrumental temperatures, and the

3 snow-energy model (*van Pelt et al*., 2012).

Year	*MP (%)*	
	Instrumental temperatures	Snow-energy model
2010	34	52
2009	55	81
2008	34	68
2007	69	78
Average	**48**	**70**

4

1 **Figures**
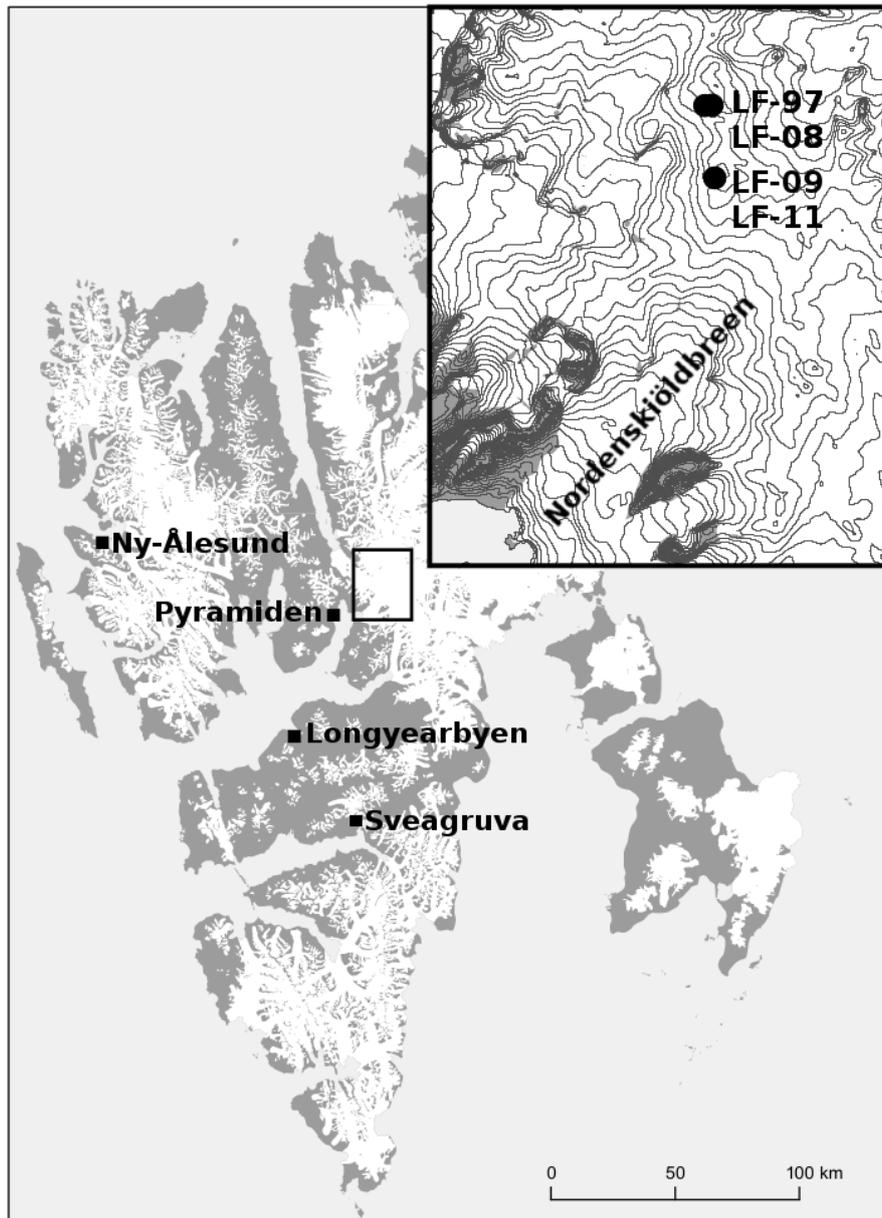
2

3 Figure 1 Map of Svalbard showing the main settlements: Longyearbyen, Ny-Ålesund and
4 Pyramiden, and the LF-97, LF-08, LF-09 and LF-11drilling sites at Lomonosovfonna.
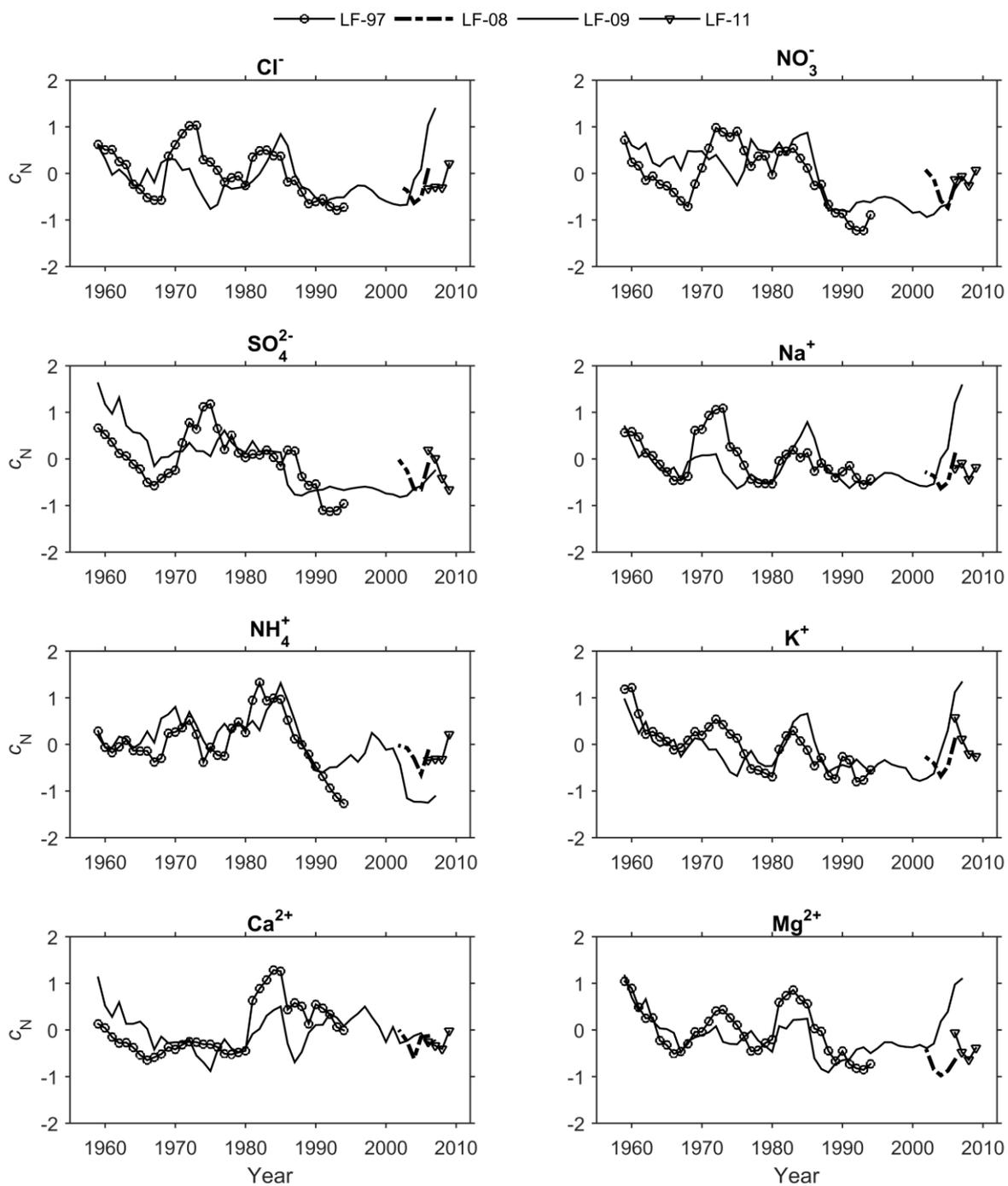
Figure 2 Comparison of normalized ionic concentrations (c_N) in the different LF-ice cores using a 5-year moving average.

1
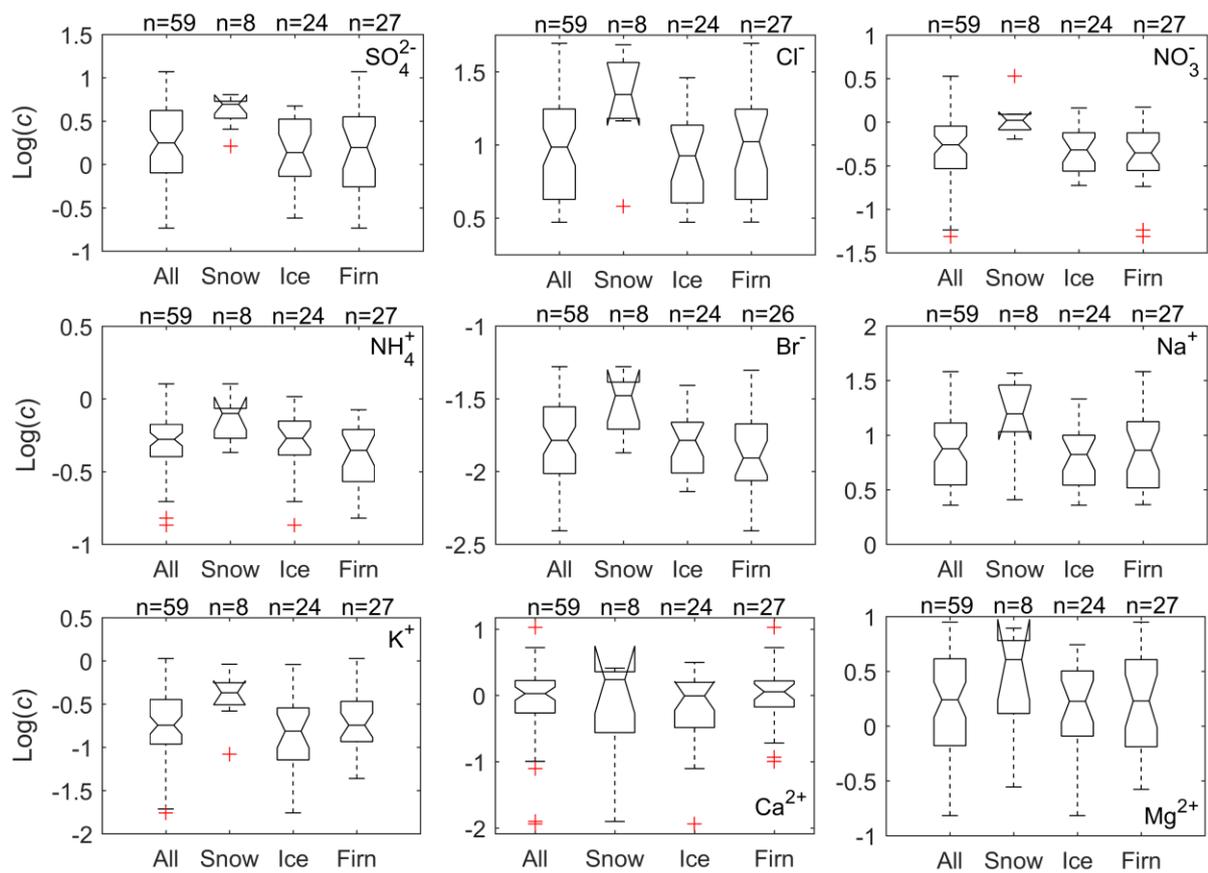
Figure 3 Box plot of log-transformed ionic concentrations (Log(*c*)) found in the different stratigraphic units in the LF-09 ice core between 2004 and 2009. *n* represents the sample size in each stratigraphic unit, and whiskers are Tukey style.

5
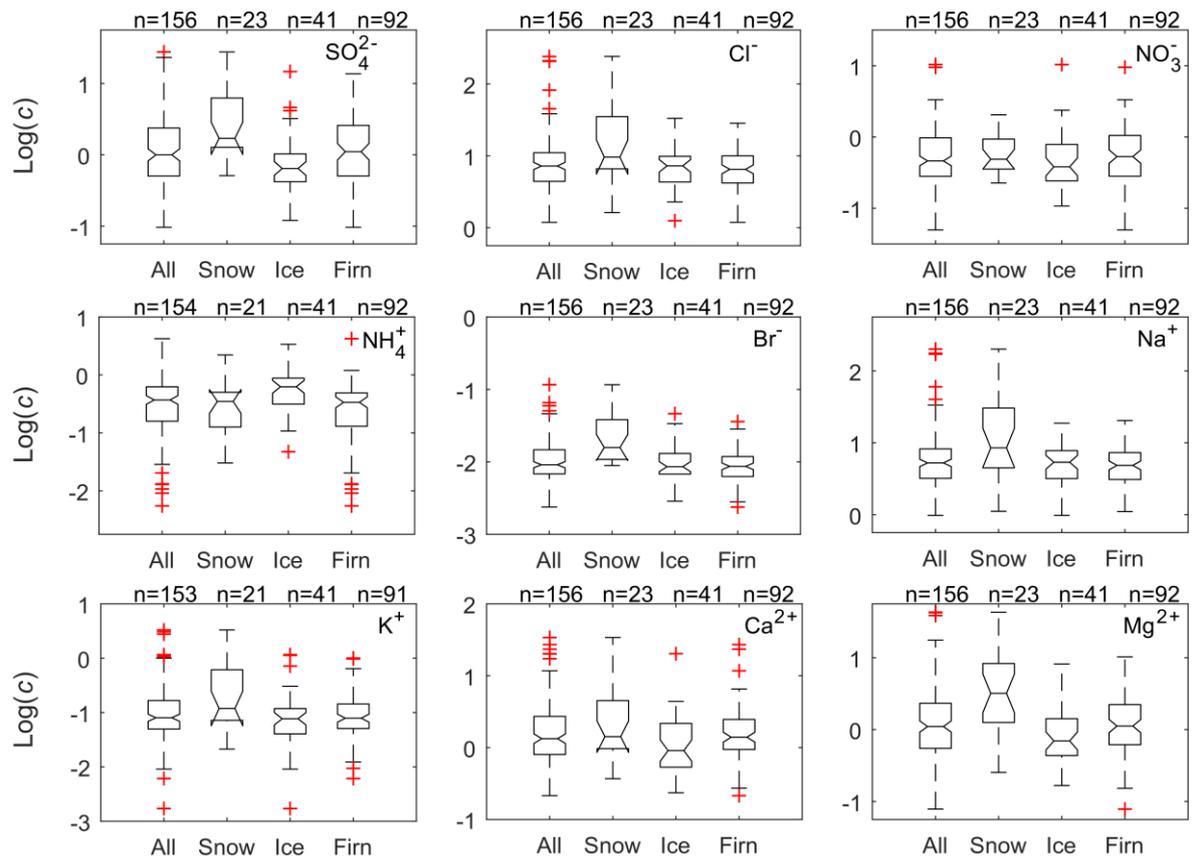
1

2   Figure 4 Box plot of ionic concentrations (Log(c)) found in the different stratigraphic units in

3   the LF-11 ice core between 2004 and 2011. *n* represents the sample size in each stratigraphic

4   unit, and whiskers are Tukey style.

5

1
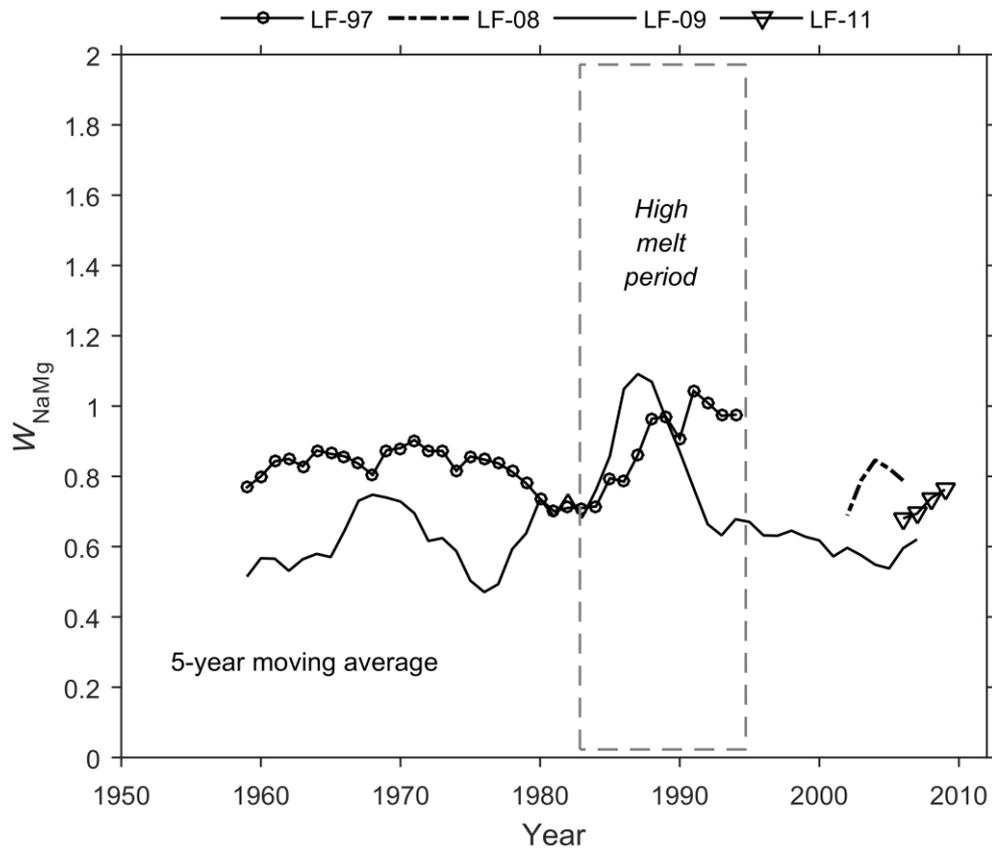
Figure 5 Melt index W_{NaMg} calculated in the different Lomonosovfonna ice cores. The values correspond to 5-year moving averages. The dashed lines indicates a high melting period during mid-80s to mid-90s.

5
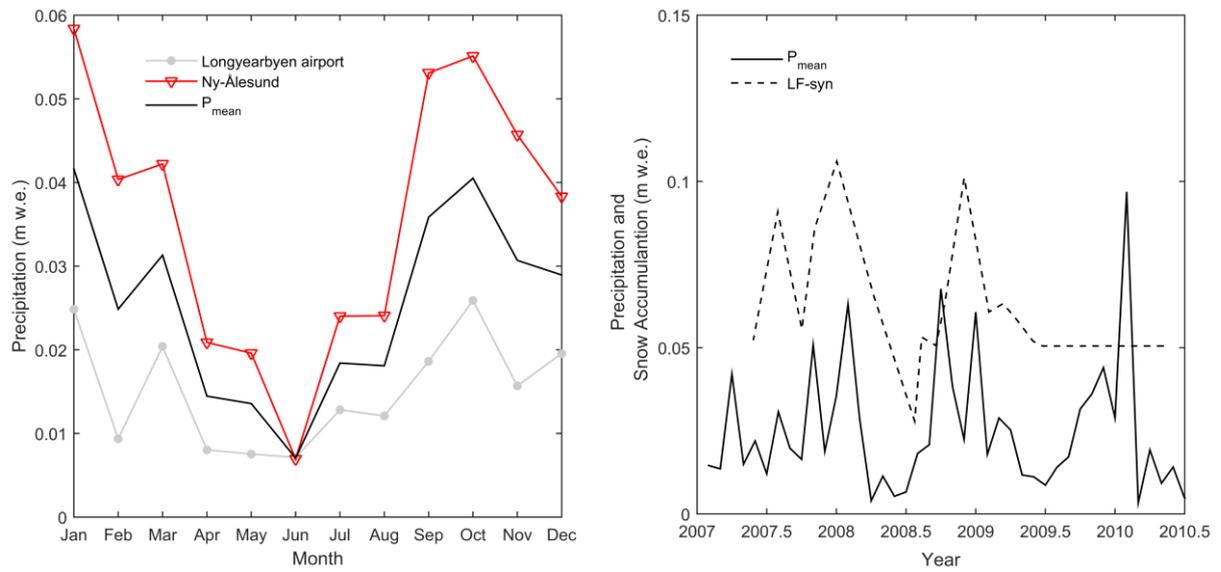
1

2 Figure 6 Annual precipitation cycle at Longyearbyen airport and Ny-Ålesund for the period

3 2007–2011 (left) and monthly precipitation amount at the stations and snow accumulation at

4 Lomonosovfonna given by the LF-syn core (right).

5

6

1
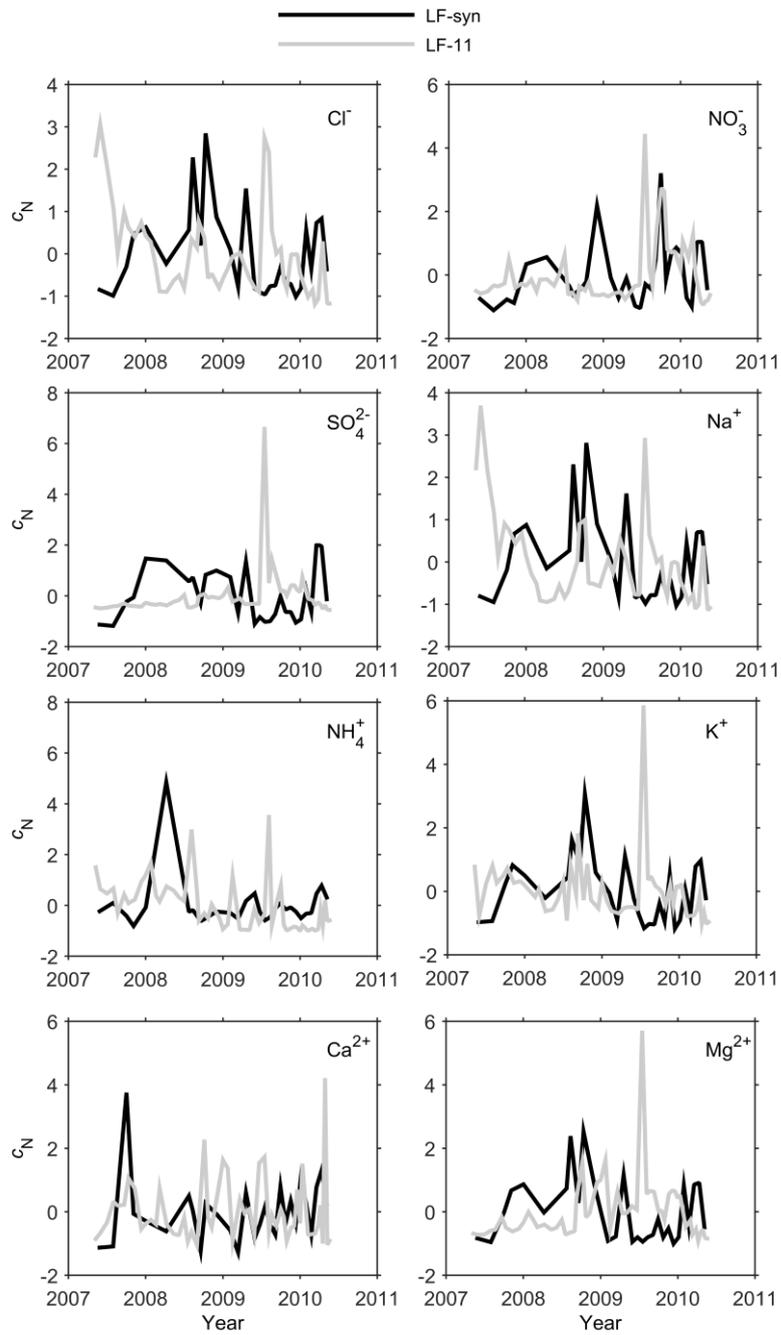
Figure 7 Comparison between a *synthetic* ice core (LF-syn, black) and the LF-11 ice core

(grey). Ionic concentrations are normalized (c_N) to mean values according to the LF-syn ice

core time scale.

5
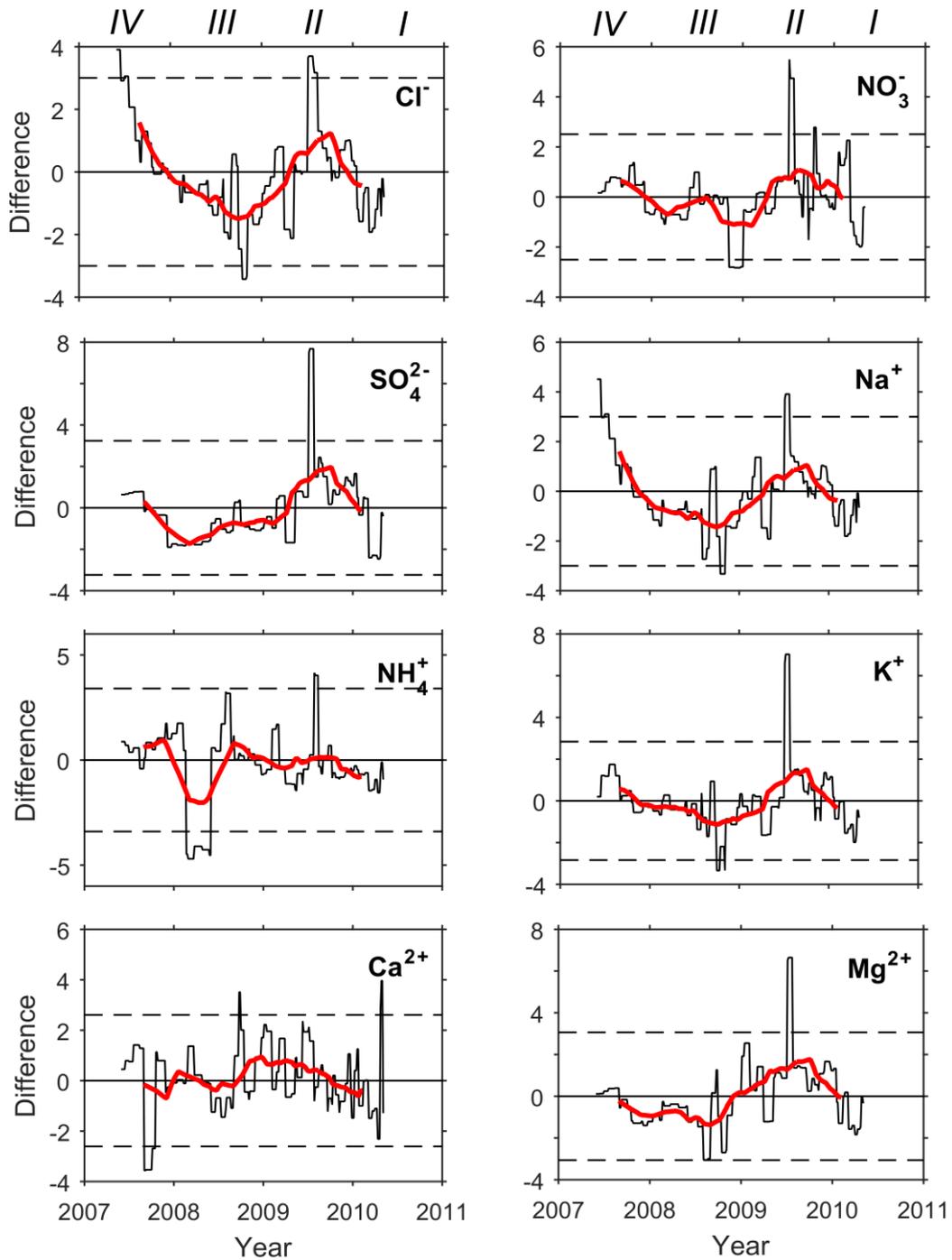
Figure 8 Difference between the normalized ionic concentrations (c_N) in the LF-11 and the LF-syn ice cores (black line). Twice the standard deviation (dashed red line) and zero values (horizontal line) are also shown. Deposition is a positive excursion and elution zones are negative excursions from the mean in each diagram. A lowpass filter (half-year moving average) is shown in red. Different periods of deposition and elution have been noted with roman numbers.
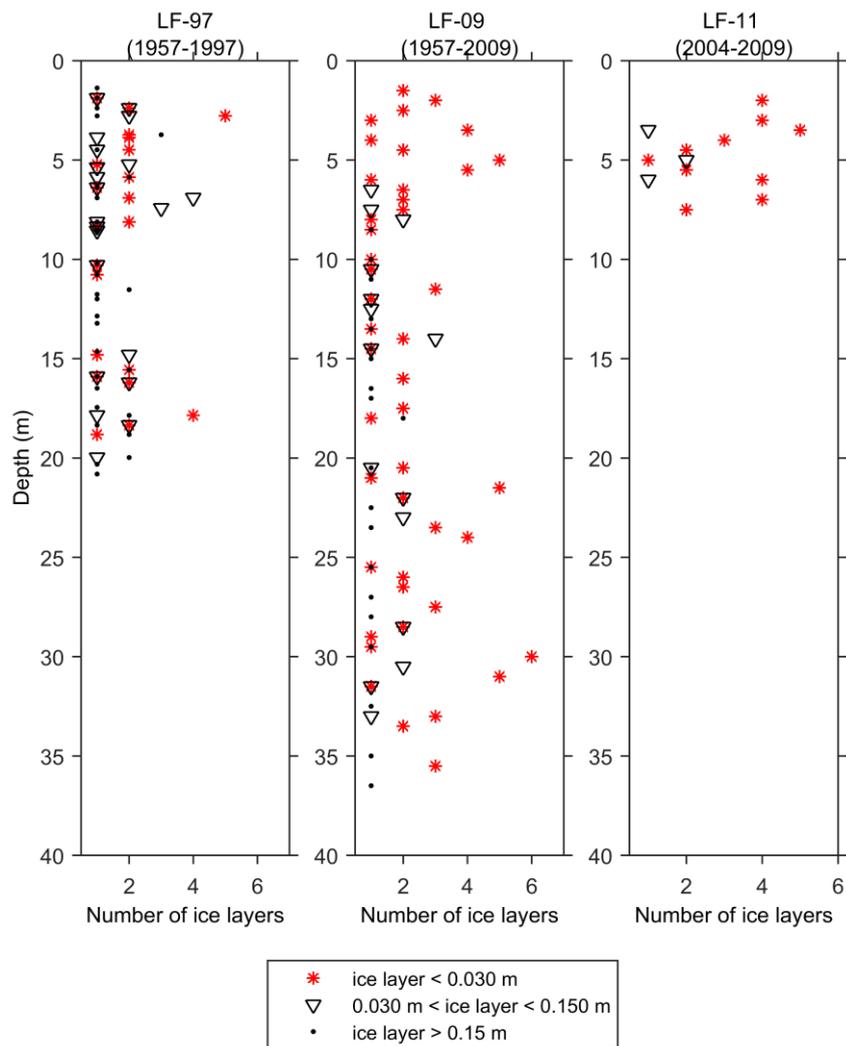
Figure 9 Number of ice layers found at different depths in the: LF-97 (left), LF-09 (centre) and LF-11 (right) ice cores. The ice layers were divided in three classes according to their thickness: thin layers (*), medium-thick layers (∇) and thick layers (●).
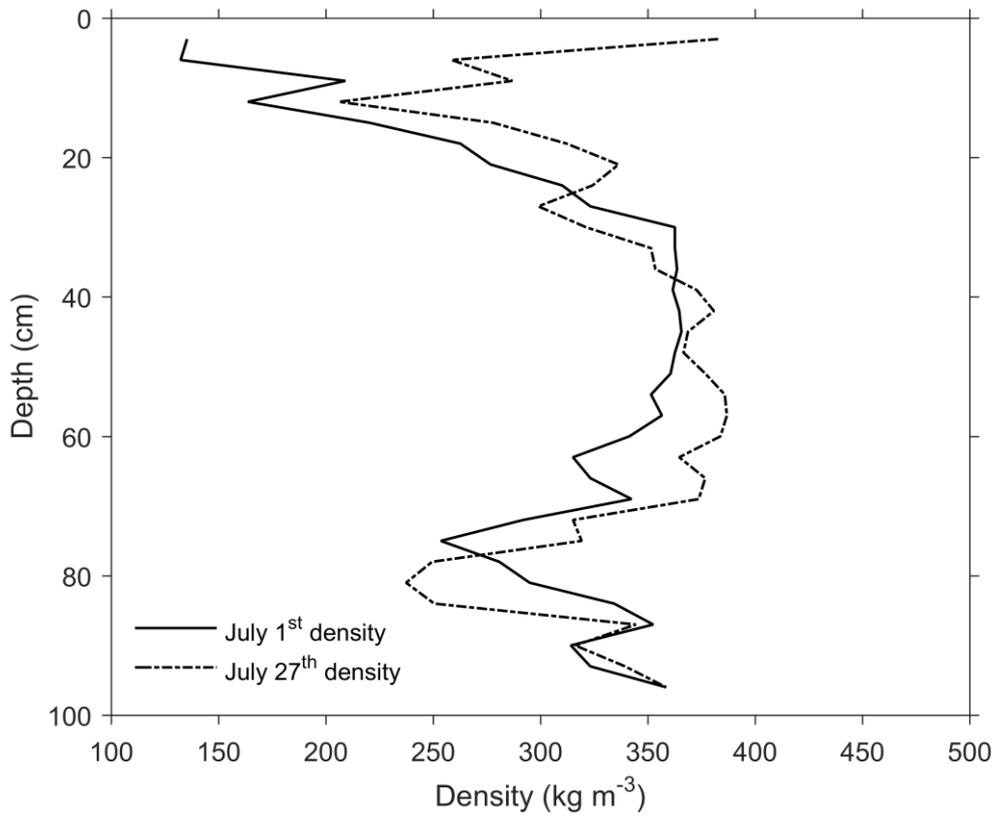
1

2   Figure 10 Density profiles in the snowpits sampled at Summit in July 1st and July 27th 2012.

3   The depth scale of the snowpit sampled in July 27th was adjusted to find a reasonable match

4   with the density profile of the snowpit sampled in July 1st.

1
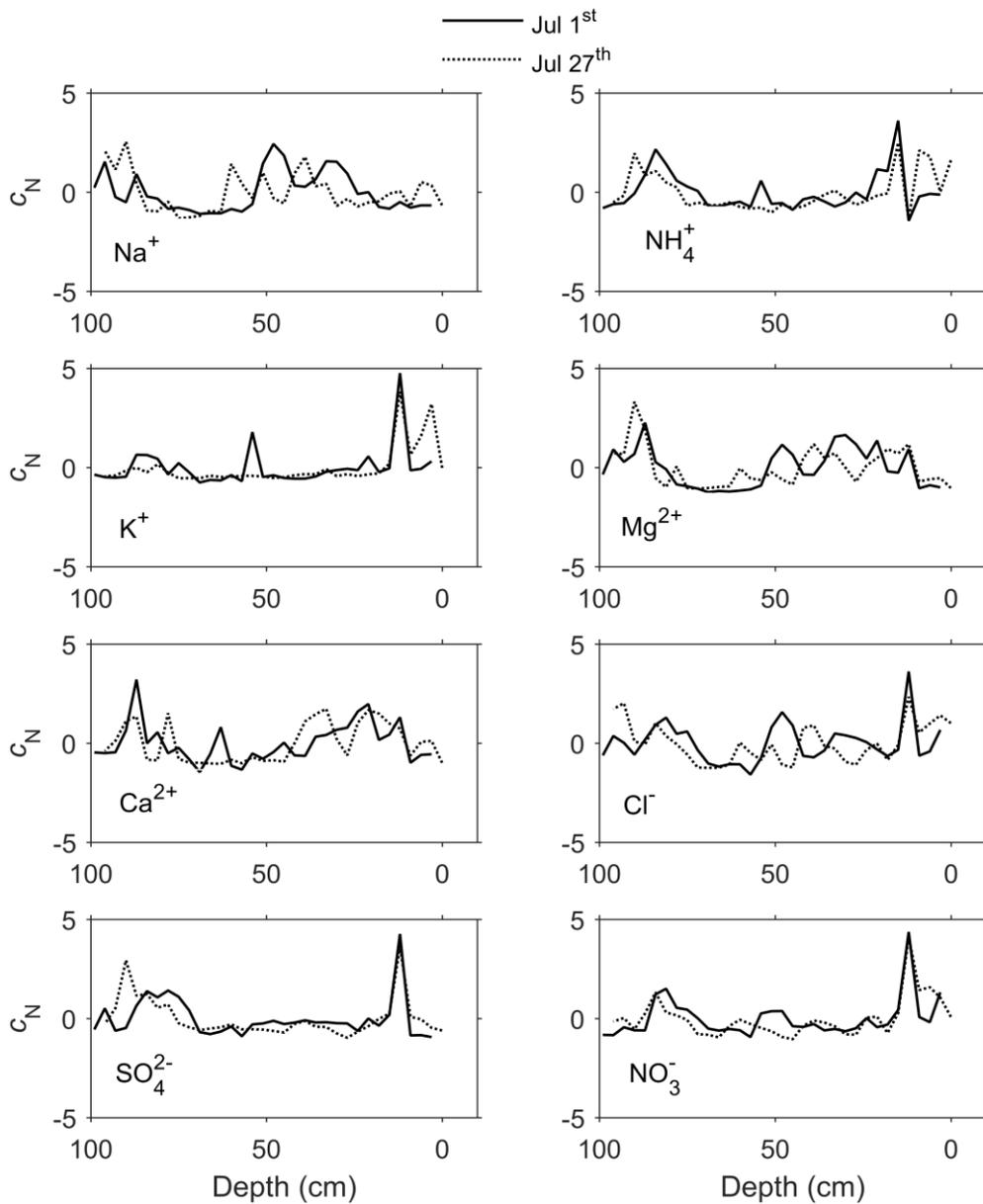
Figure 11 Comparison between the snowpit sampled in July 1st 2012 and the snowpit sampled

in July 27th 2012. Ionic concentrations are normalized (c_N).

1
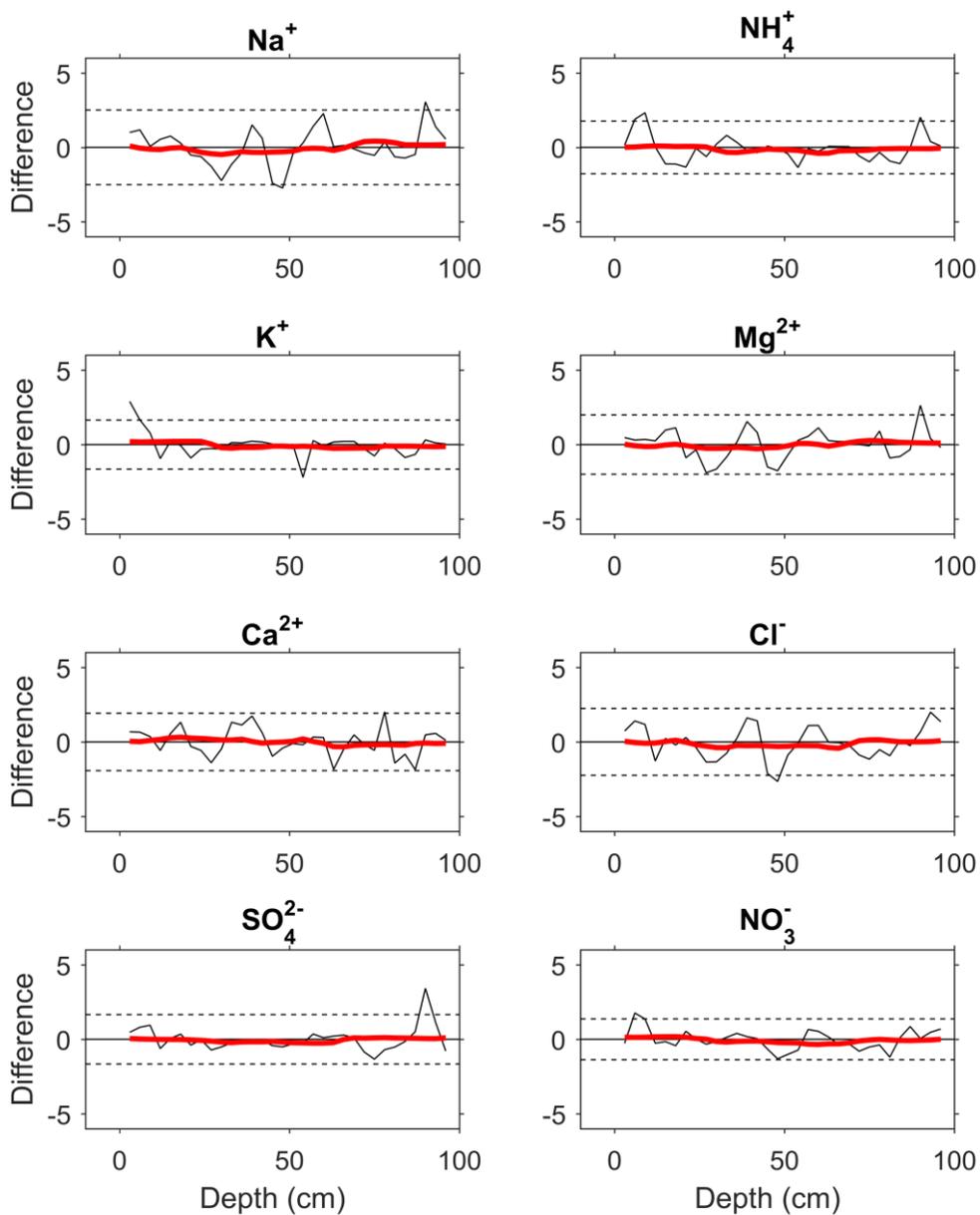
Figure 12 Difference between the normalized ionic concentrations (c_N) in the snowpit
sampled in July 27th 2012 and July 1st 2012. Twice the standard deviation and zero values are
also shown. Deposition is a positive excursion and elution zones are negative excursions from
the mean in each diagram.
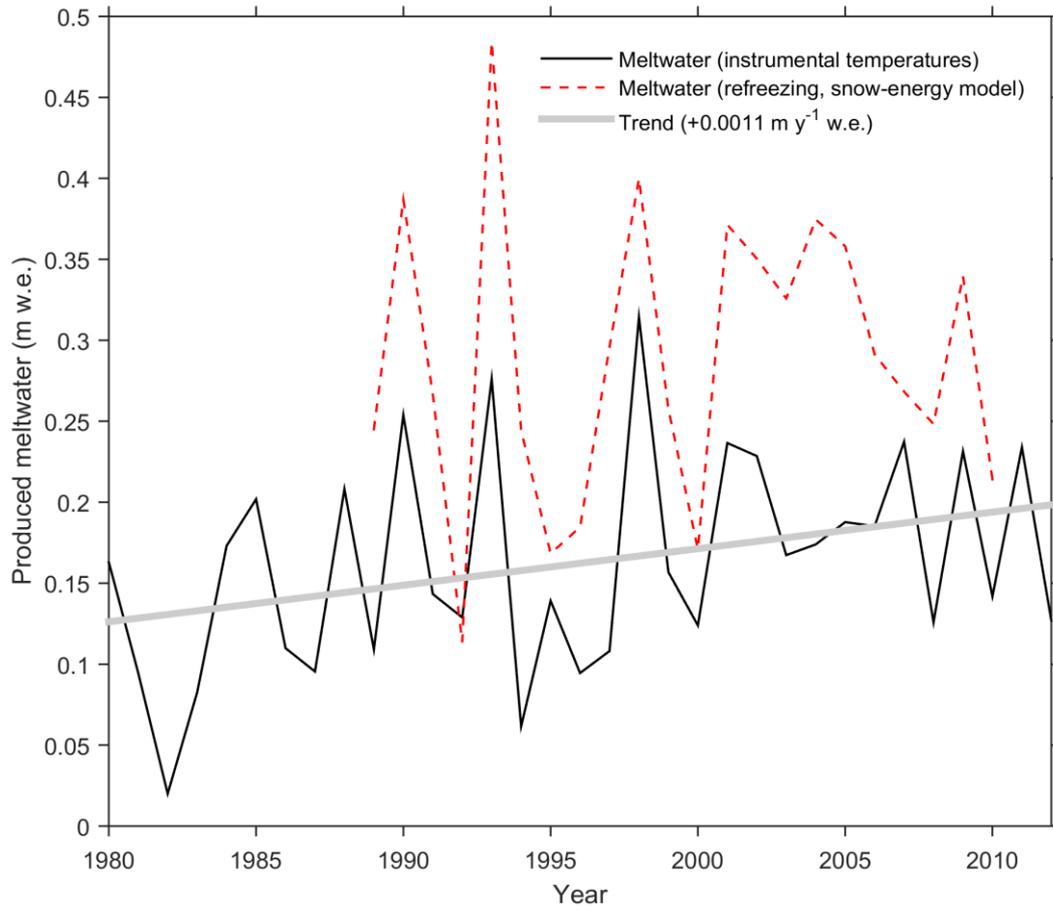
1

2   Figure 13 Produced meltwater calculated at Lomonosovfonna using the PDD (black) and

3   snow-energy model (dashed red) approaches. The linear trend of meltwater calculated with

4   the PDD approach and instrumental temperatures is also shown over the 1979–2012 period

5   (grey).

6
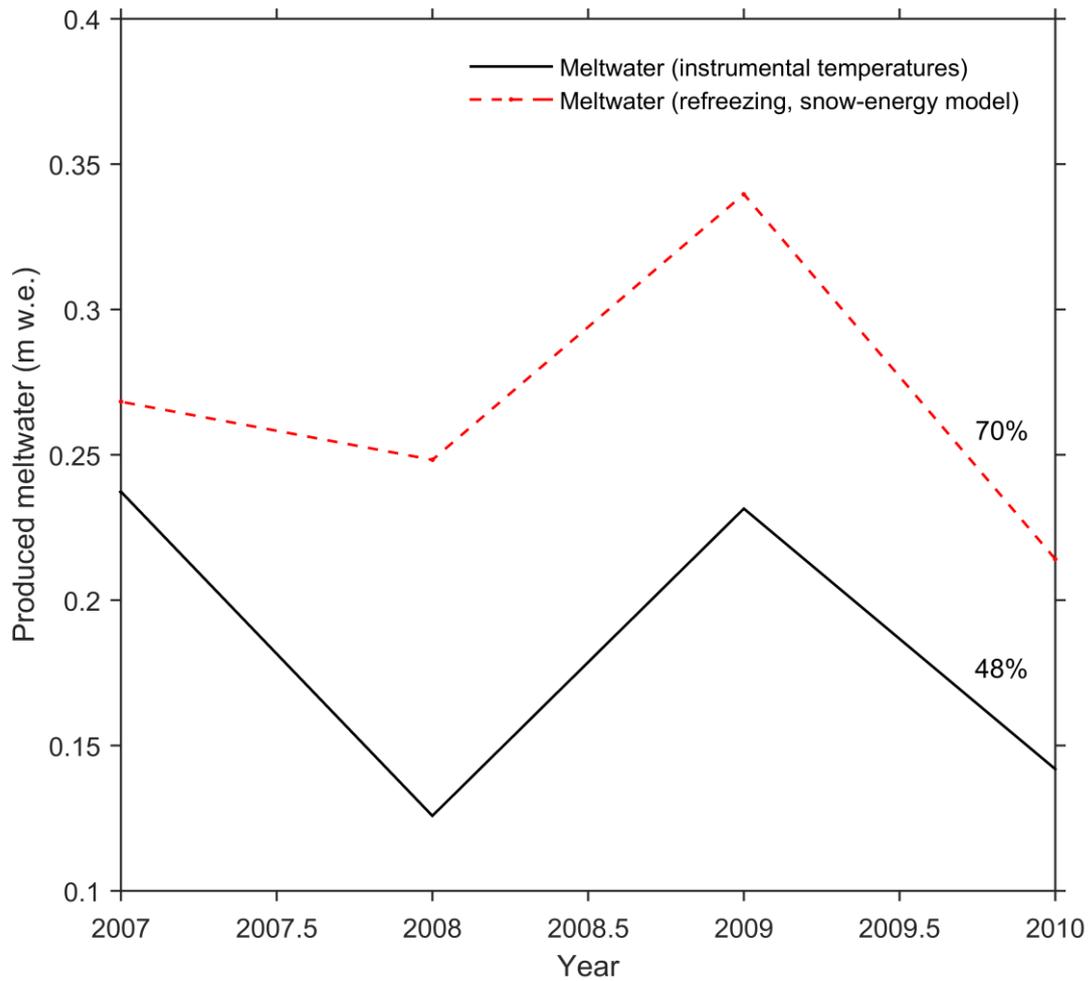
1

2　Figure 14 Meltwater calculated at Lomonosovfonna during the period 2007–2010 using the

3　different approaches: PDD and instrumental temperatures (black); and the snow-energy model

4　(dashed red). The percentages above each line represent the average melt percentage (MP)

5　during the studied period, estimated by the different approaches.

6
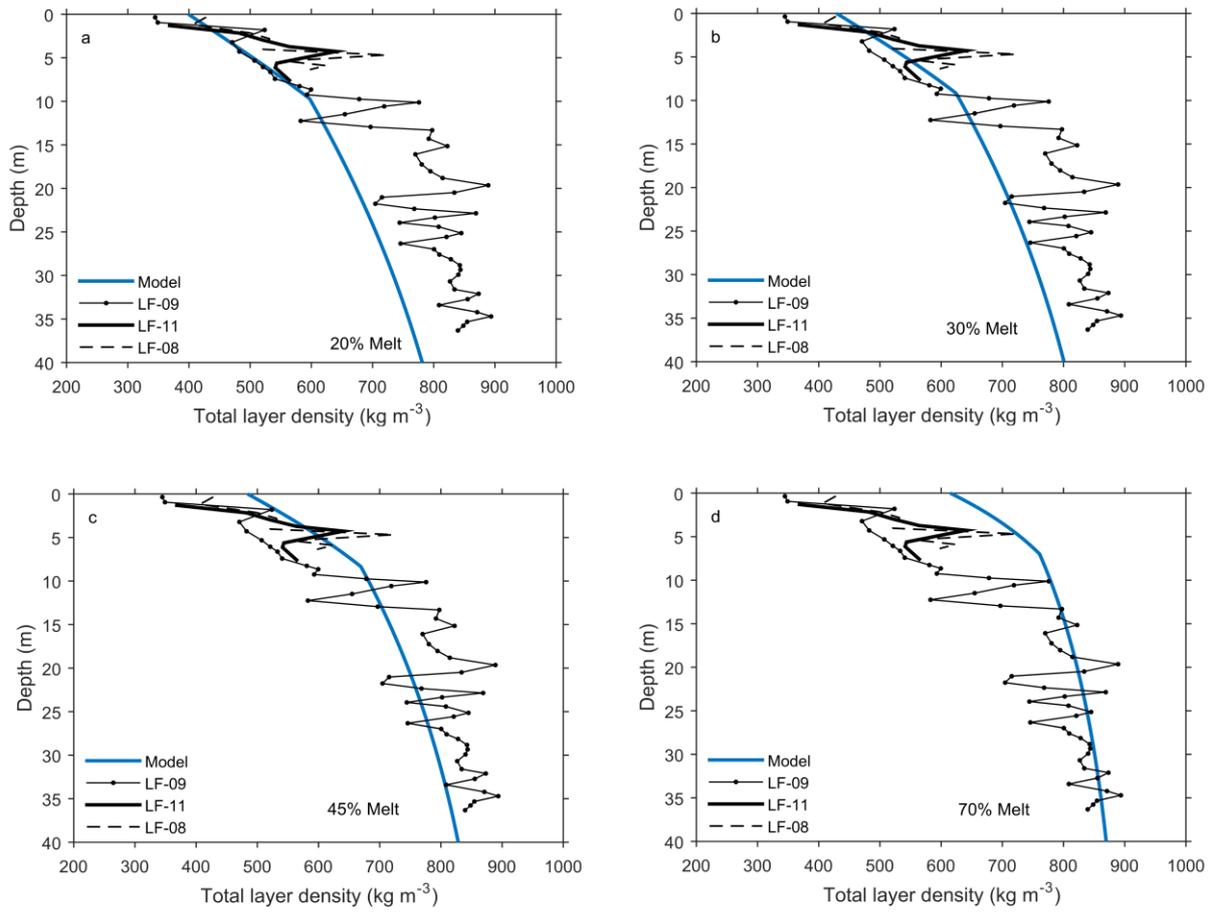
1

2   Figure 15 Comparison between the LF-08, LF-09 and LF-11 ice core density profiles (annual

3   averages) and the output of the firn-densification model (*Reeh et al.* 2005), considering: a)

4   20% of melt, b) 30% of melt, c) 45% of melt, and d) 70% of melt.

5
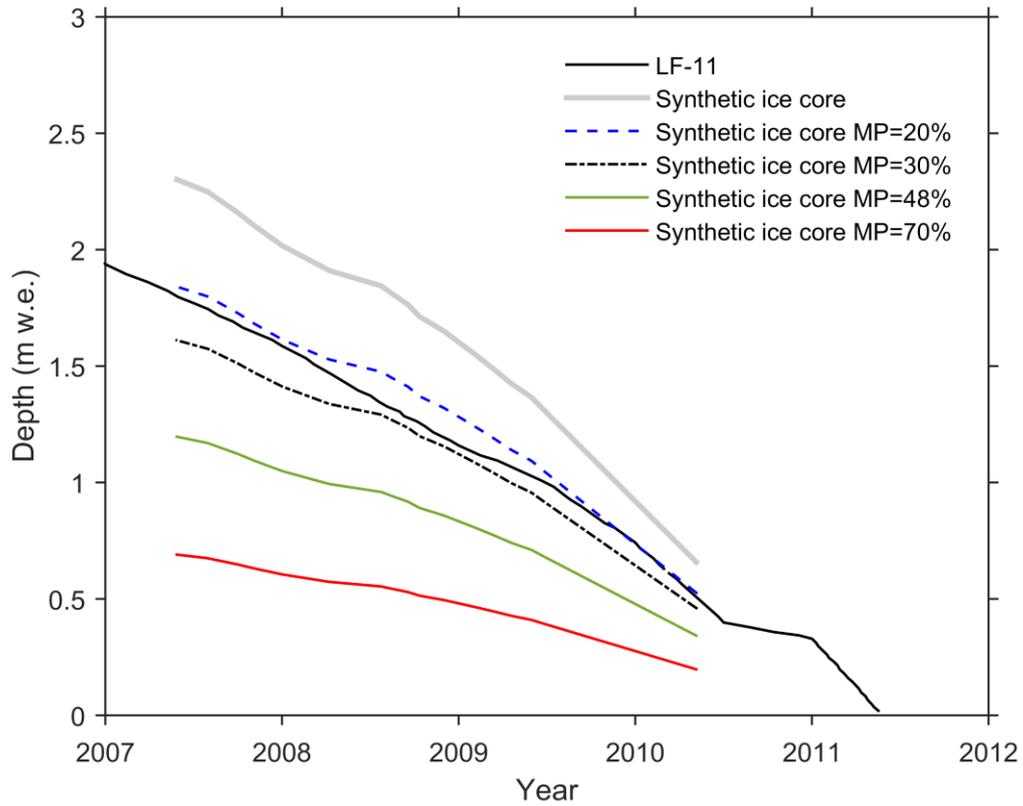
Figure 16 Depth–time scales for the LF-11 and LF-syn ice cores during 2007–2011 (black and grey lines, respectively). Blue dashed, black-dot-dashed, green and red lines represent the synthetic core depth–time scale considering a MP of 20 %, 30 %, 48 % and 70 %, respectively.